A time-calibrated species tree phylogeny of the New World Cycad genus Zamia L. (Zamiaceae, Cycadales)

Calonje, Michael ; Meerow, Alan W ; Griffith, M Patrick ; Salas-Leiva, Dayana ; Vovides, Andrew P ; Coiro, Mario ; Francisco-Ortega, Javier

DOI: https://doi.org/10.1086/702642

Int. J. Plant Sci. 180(4):000–000. 2019.
1058-5893/2019/18004-00XX$15.00 DOI: 10.1086/702642

A TIME-CALIBRATED SPECIES TREE PHYLOGENY OF THE NEW WORLD CYCAD GENUS *ZAMIA* L. (ZAMIACEAE, CYCADALES)

Michael Calonje,[1,*,†] Alan W. Meerow,[‡] M. Patrick Griffith,[†] Dayana Salas-Leiva,[*,‡,**] Andrew P. Vovides,[§] Mario Coiro,[‖] and Javier Francisco-Ortega[*,#]

*Department of Biological Sciences, Florida International University, Miami, Florida 33199, USA; †Montgomery Botanical Center, Coral Gables, Florida 33156, USA; ‡USDA ARS Subtropical Horticultural Research Station, Miami, Florida 33158, USA; §Instituto de Ecología, A.C., Xalapa, Veracruz 91000, Mexico; ‖Department of Systematic and Evolutionary Botany, University of Zurich, Switzerland; #Fairchild Tropical Botanic Garden, Coral Gables, Florida 33156, USA; and **Centre for Comparative Genomics and Evolutionary Bioinformatics, Department of Biochemistry and Molecular Biology, Dalhousie University, Halifax, Nova Scotia B3H 4R2, Canada

Editor: Hervé Sauquet

Premise of research. The genus *Zamia* L. (Zamiaceae), consisting of 79 species, is the most species-rich and widely distributed cycad genus in the New World and arguably the most morphologically and ecologically diverse genus in the Cycadales. However, a strong phylogenetic framework for this genus is still lacking.

Methodology. We used a multilocus sequence data set of 10 independent loci (nine single-copy nuclear genes [SCNGs] and one plastid) and extensive taxon sampling (ca. 90% of species) to infer phylogenetic relationships within *Zamia*. We implemented a concatenated matrix analysis with maximum parsimony, a partitioned maximum likelihood (ML) analysis, and a time-calibrated Bayesian species tree-estimation approach. Diversification, historical biogeography, and ancestral character state reconstruction analyses were conducted using the species tree topology that was the most morphologically and geographically congruent.

Pivotal results. We inferred a robust phylogenetic tree for the genus with a strong geographic delimitation of clades and found that four morphological characters typically used for diagnostic purposes in the genus exhibit a high degree of homoplasy. The stem group of *Zamia* was estimated to have originated at 68.28 Ma (95% highest posterior density [HPD] 51.0–84.5) and the crown group at 9.54 Ma (95% HPD 9.0–10.62). The majority of species richness in the genus appeared during the Pliocene and Pleistocene, with the highest diversification rates occurring in clades comprising Caribbean and South American species. Biogeographic analysis suggests a Caribbean or Mesoamerican origin for *Zamia* with subsequent dispersal to the Central American Isthmus and South America, where the genus reaches its maximum species and morphological diversity.

Conclusions. The high degree of convergence found in multiple morphological characters has historically confounded efforts to elucidate species relationships using nonphylogenetic methods. This study presents the most species-comprehensive, well-resolved hypothesis of phylogenetic relationships within *Zamia* and provides a strong phylogenetic framework for further studies.

Keywords: cycads, biogeography, gymnosperms, diversification.

Online enhancements: appendixes.

Introduction

The genus *Zamia* L. (Zamiaceae, Cycadales) is widely considered to be the most ecologically and morphologically diverse genus of the extant cycads (Norstog and Nichols 1997). With its 79 accepted species (Calonje et al. 2019), it is the most species-rich and broadly distributed genus among the New World genera of the Zamiaceae. It is restricted primarily to the Neotropical region (sensu Sclater 1858; Morrone 2014) with only the northernmost *Zamia integrifolia* L.f. populations in Florida and southeast Georgia extending into the Nearctic region (sensu Escalante et al. 2013; Morrone 2014). The distribution of the genus can be spatially divided into three separate areas of endemism: (1) a Caribbean group restricted to islands on the Bahama Archipelago and Greater Antilles, as well as to the mainland states of Florida and Georgia in the southeastern United States, (2) a Mesoamerican group extending from Tamaulipas, Mexico, to northern El Salvador, and (3) a Central

[1] Author for correspondence; email: michaelc@montgomerybotanical.org.

Manuscript received July 2018; revised manuscript received October 2018; electronically published April 2, 2019.

and South American group occurring from southern Nicaragua to Bolivia, the southernmost extent of the genus (fig. 1).

Despite the remarkable species diversity and broad geographic distribution of *Zamia*, the only formal infrageneric classification of the genus was published decades ago in Schuster's (1932) monograph of cycads. Schuster included 26 species in his treatment of *Zamia* and divided the genus into three geographically defined sections (Caribaeae, Mexicano-Meridionales, and Centrali-Meridionales) that are broadly congruent with the Caribbean, Mesoamerican, and Central and South American species groups outlined above. However, Schuster did not designate types for these sectional names, making their taxonomic application uncertain. Furthermore, several of Schuster's proposed sectional names are illegitimate because they included the type of the name of the genus and did not repeat the generic name unaltered as its epithet, as required by nomenclatural rules (art. 22.1, Turland et al. 2018). Such is the case with Schuster's "Caribbaeae," which is illegitimate because it includes the type of the genus (*Zamia pumila* L.) and had to be called section *Zamia* to be considered a legitimate name. Schuster's work is also notorious for contravening the rules of priority and other nomenclatural rules, and it includes very elaborate and often nonsensical infraspecific hierarchies (see Johnson 1959; Hill 1996). Consequently, Schuster's classification has been disregarded by most

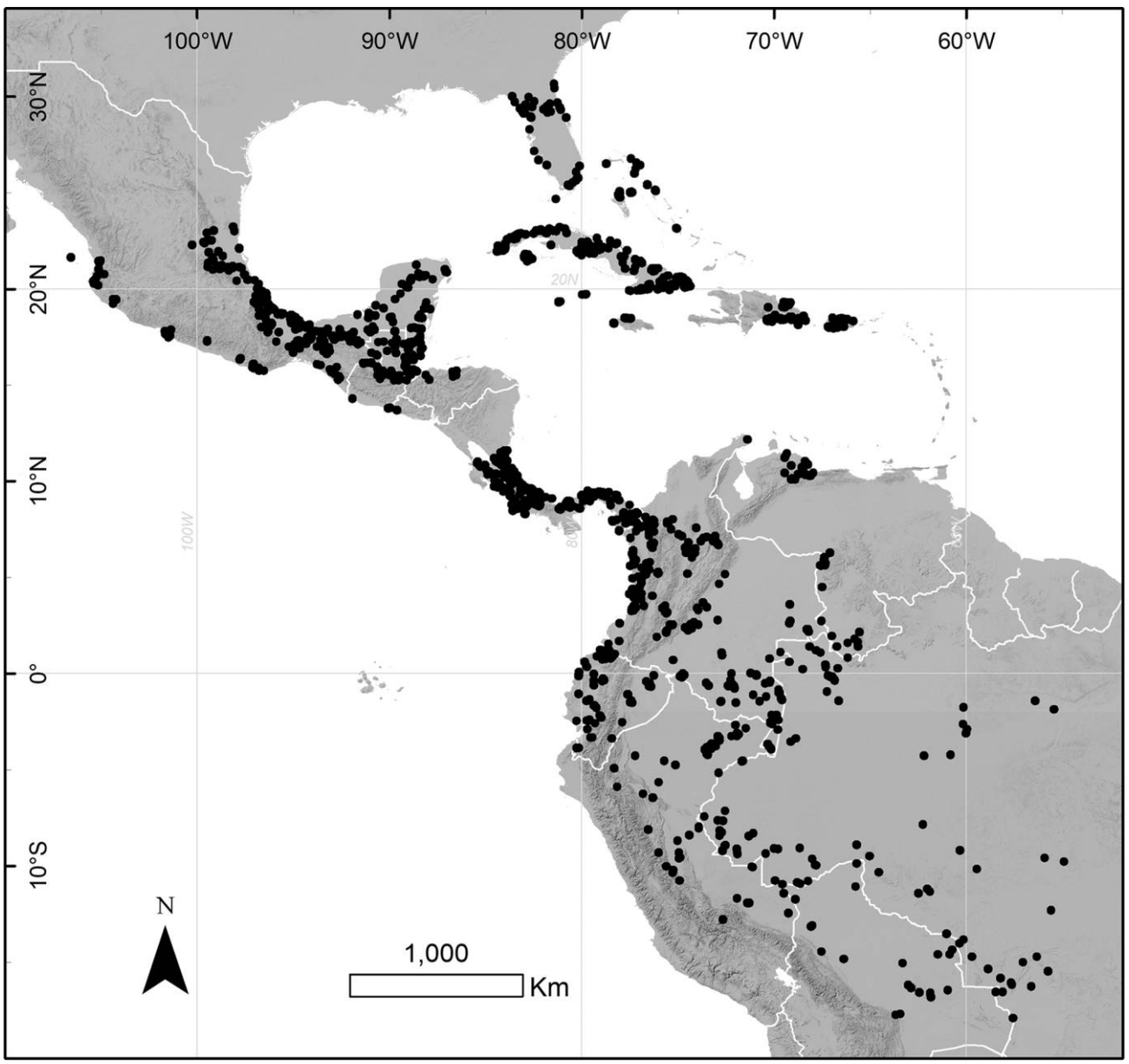

Fig. 1 Geographic distribution of the New World endemic genus *Zamia*. Occurrence data were compiled from 2594 herbarium specimens and observation records derived from M. Calonje's research database. Notice the disjunctive Caribbean, Mesoamerican, and Central and South American geographic groupings.

authors, although some of Schuster's sectional names have been typified and adopted in formal classification work, most notably in *Cycas* (see Hill 1995). However, no authors since Schuster have attempted formal classification of supraspecific taxa within *Zamia*. Subsequent authors have instead mostly limited themselves to informally classifying and surmising interspecific relationships within subsets of the genus based on similarities in geographic distribution (Norstog and Nichols 1997), morphology (e.g., Schutzman et al. 1988; Taylor et al. 2008; Calonje et al. 2010, 2011), anatomy (Acuña-Castillo and Marín-Méndez 2013), karyology (Caputo et al. 1996), genome sizes (Zonneveld and Lindström 2016), and other characters. Nevertheless, the phylogenetic relationships within the genus remain unclear, as only a limited number of studies have involved a species-level phylogenetic component.

Most notably, Caputo et al. (2004) conducted a phylogenetic analysis of *Zamia*, including 23 of the 79 currently accepted species in a parsimony-based phylogenetic analysis of sequences of the internal transcribed spacer 2 of nuclear ribosomal DNA in combination with a morphological data set. The analysis found several clades to be more congruent with geographic distribution than with morphological similarities, leading the authors to suggest that convergent evolution of morphological characters is pervasive in the genus. Geographically congruent clades identified included those composed of Central American, North American, and Caribbean species, as well as a combined clade including South American and Central American species (fig. 2*A*).

Clugston et al. (2016) examined the phenological phases of 11 species of *Zamia* in a phylogenetic context, presenting a tree based on a maximum parsimony (MP) analysis using nucleotide sequence data from two plastid genes (*matK*, *rbcL*), two SCNGs (*CAB*, *NEEDLY*), and one high-copy nuclear gene (*26S*). This analysis showed strong support for a Caribbean clade and a monophyletic South American group, and moderate support for a Central American lineage (fig. 2*B*).

To examine the diversification ages of extant cycads, Nagalingum et al. (2011) used the nuclear gene phytochrome P (*PHYP*) with a few additional sequences from the chloroplast genes *matK* and *rbcL* to produce a time-calibrated phylogeny of 199 taxa, including 31 species of *Zamia*. The results indicated that most living cycad species are the result of quite recent diversification of a very ancient lineage and are therefore much younger than previously thought. This was suggested previously by Treutlein and Wink (2002) in an earlier phylogenetic study using *rbc*L plastid sequences and also found to apply generally to extant gymnosperms by Crisp and Cook (2011). Although infrageneric relationships were not discussed by Nagalingum et al. (2011), their phylogeny supported the monophyly of *Zamia*, albeit with low node support throughout most of the genus (fig. 2*C*). Similarly, in an article using the same molecular markers but with the inclusion of additional species and fossil calibration constraints, Condamine et al. (2015) also found poor node support within genera. Although both divergence time estimation studies included a large number of cycad species in their analyses, they similarly obtained generally low node support within genera, which was likely due to the sparse and often nonoverlapping locus sampling between species and the limited informative sites present in the markers selected.

As illustrated above, the phylogenies published to date that focus on *Zamia* or contain a considerable sampling of the genus are of limited utility due to low taxon sampling (e.g., Clugston et al. 2016) and/or weak phylogenetic information resulting from a small number of molecular markers (e.g., Caputo et al. 2004; Nagalingum et al. 2011). In this article, we use a larger multilocus sequence data set of 10 independent loci (nine SCNGs and one plastid) and extensive taxon sampling (>90% of species) to infer phylogenetic relationships within the genus *Zamia* using MP, ML, and Bayesian time-calibrated species-tree inference methods. We discuss our results in the context of clade age estimation, diversification, ancestral character state reconstruction, and biogeographical history.

Material and Methods

Taxonomic Sampling

DNA was isolated from 113 individual leaflet samples of *Zamia* belonging to 70 of the 79 currently accepted species in the genus (Calonje et al. 2018) and from single samples of *Microcycas calocoma* (Miq.) A.DC. and *Stangeria eriopus* (Kunze) Baill. that were included as outgroups for phylogenetic analyses. Multiple samples were collected for some species of *Zamia*, particularly from those with broader geographic distributions. The leaflet samples were obtained primarily from plants of known provenance or pedigree cultivated in botanic gardens and other botanical collections (app. A).

Outgroup Selection

Microcycas calocoma and *Stangeria eriopus*, both belonging to monotypic genera, were selected as outgroups for phylogenetic analyses, with the latter as the functional outgroup. *Microcycas* is strongly supported as the sister genus to *Zamia* and *Stangeria* as sister to *Zamia* + *Microcycas* in a recent genus-level phylogeny of the Cycadales that used multiple phylogenetic methods (Salas-Leiva et al. 2013) as well as in other phylogenetic studies (e.g., Rai et al. 2003; Bogler and Francisco-Ortega 2004; Chaw et al. 2005; Zgurski et al. 2008).

Marker Selection

Sequences of nine independent, cycad-specific SCNGs and one chloroplast gene (table 1) were used to infer the phylogeny of the genus *Zamia* using various phylogenetic methods. Of the markers used, seven (*40S*, *ATG2*, *GroES*, *HTS*, *LiSH*, *PEX4*, *PMP22*, *WRKY4*) were identified and developed in our laboratories (Salas-Leiva et al. 2014); the remaining ones (*CyAG*, *psbK/I*) were derived from previous publications (table 2). The loci *40S*, *ATG2*, *CyAG*, and *GroES* were previously used to infer the generic relationships of the Cycadales (Salas-Leiva et al. 2013), and *40S*, *ATG2*, *CyAG*, *GroES*, *LiSH*, *PEX4*, and *WRKY4* were applied to assess the genetic diversity and genetic structure of Bahamian zamias (Salas-Leiva et al. 2017). The single chloroplast gene locus included in the study (*psbK/I*) was selected because it had displayed the best performance (amplification success and high no. diagnostic sites) in a previous work that evaluated seven different chloroplast genes for barcoding Mexican species of *Zamia* (Nicolalde-Morejón et al. 2011).

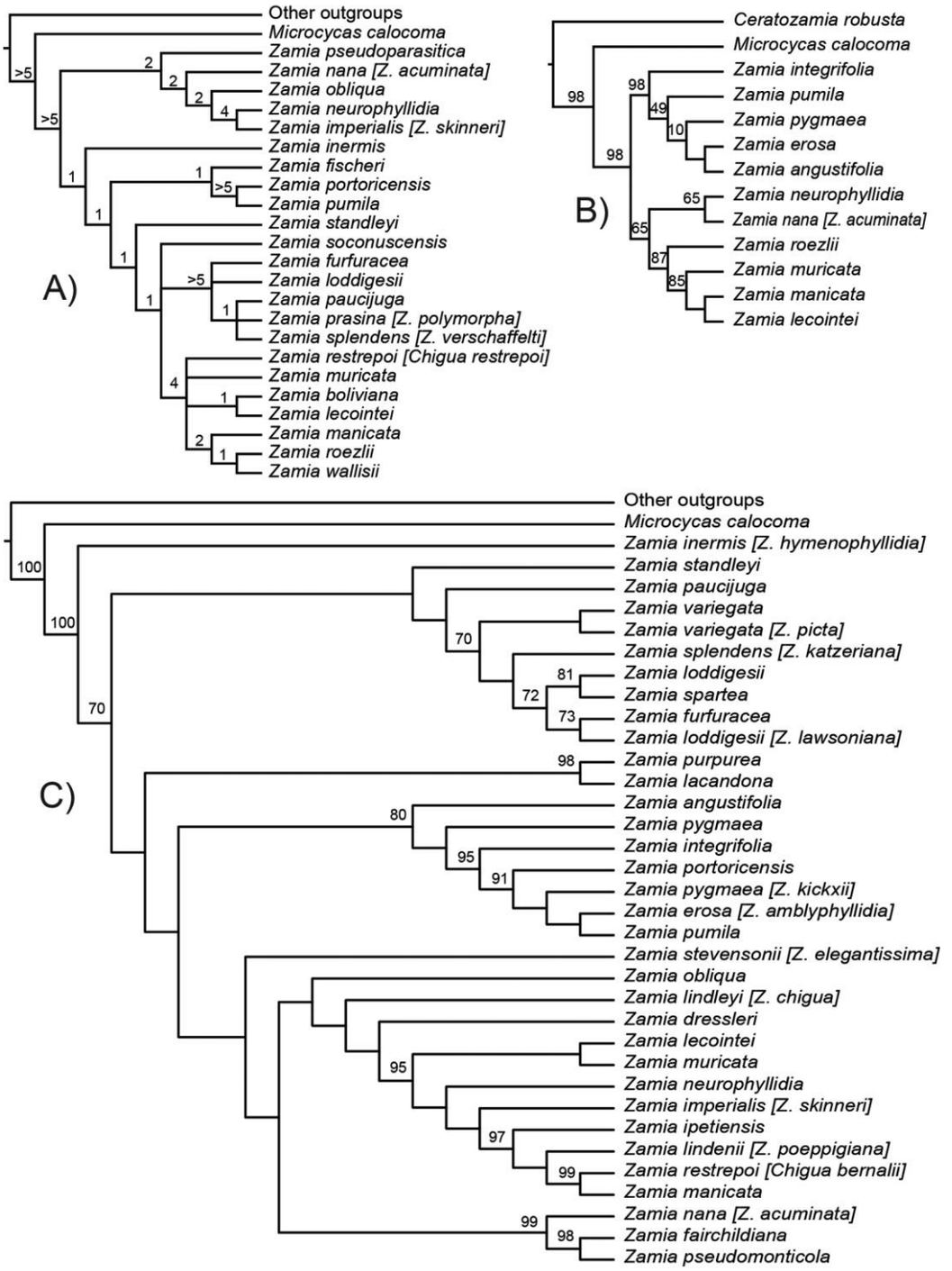

Fig. 2 Phylogenetic tree topologies for *Zamia* resolved by other authors. Some taxon names are revised based on current taxonomy and nomenclature; original names are shown in brackets. *A*, Caputo et al. (2004): Maximum parsimony consensus tree using combined morphological data and nrDNA *ITS2*; numbers above branches indicate branch support (up to five-step-longer trees). *B*, Clugston et al. (2016): Maximum parsimony strict consensus tree found using combined nuclear (*26S*, *CAB*, *NEEDLY*) and plastid (*matK*, *rbcL*) genes; numbers above branches are jackknife support values. *C*, Nagalingum et al. (2011): Maximum likelihood tree generated from concatenated matrix combining one nuclear (*PHYP*) and two plastid (*matK*, *rbcL*) genes; numbers above branches are bootstrap support values above 70%.

Table 1

Locus Name, Description, and Publication Source for Foci Used in This Study

Locus ID	Locus description	Reference(s)
40S	40S ribosomal protein S27-2 (RS27A)	Salas-Leiva et al. 2014
CyAG	MADS-box transcription factor family AGAMOUS	Zhang et al. 2004, Salas-Leiva et al. 2013
ATG2	ATG2, EBP1, ATEBP1, metallopeptidase M24 family protein	Salas-Leiva et al. 2014
GroES	GroES-like zinc-binding alcohol dehydrogenase family protein	Salas-Leiva et al. 2013
HTS	Histidyl-tRNA synthetase	Salas-Leiva et al. 2013
LiSH	LisH/CRA/RING-U-box domain-containing protein	Salas-Leiva et al. 2014
PEX4	PEX4, peroxin4	Salas-Leiva et al. 2014
PMP22	Peroxisomal membrane 22 kDa (Mpv17/PMP22) family protein	Salas-Leiva et al. 2014
WRKY4	WRKY transcription factors	Salas-Leiva et al. 2017
psbK/I	Noncoding intergenic chloroplast spacer	Lahaye et al. 2008

DNA Extraction, Amplification, and Sequencing

DNA was extracted from 20 to 100 mg of fresh or silica-gel-desiccated leaflet tissue using the FastDNA spin kit (MP Biomedicals, Santa Ana, CA) and the FastPrep-24 instrument (Qbiogene, CA). The extracted DNA was quantified using a GeneQuant Pro RNA/DNA calculator-spectrophotometer (GE Healthcare Life Sciences) or NanoDrop 2000 spectrophotometer (Thermo Scientific) and diluted to 10 ng/μL. Amplifications contained 1× amplification Buffer with 2 mM $MgSO_4$, 10 mM of dNTPs, 0.2 mg/mL bovine serum albumin, 10 μM of forward and reverse primer, 0.05 U/μL Taq DNA polymerase (New England BioLabs, Ipswich, MA), and 10 ng/μL of template DNA brought to a total volume of 15 μL with nuclease-free H_20. DNA samples were amplified using C1000 and S1000 thermal cyclers (Bio-Rad Laboratories, Hercules, CA). Most genes were amplified in single fragments, with the exception of *CyAG* and *GroES*, which were each amplified in two separate fragments using separate primer pairs. For all loci except *GroES*, the following thermal profile was used: 95°C for 2 min, 35 cycles of 95°C for 30 s, annealing temperature (50°–60°C) for 1 min, 72°C for 1 min, and a final extension at 72°C for 7 min. Both fragments of the locus *GroES* were amplified using touchdown PCR (95°C for 2 min; three cycles of 95°C for 30 s, 55°C for 1 min, 72°C for 1 min; three cycles of 95°C for 30 s, 54°C for 1 min, 72°C for 1 min; three cycles of 95°C for 30 s, 53°C for 1 min, 72°C for 1 min; three cycles of 95°C for 30 s, 52°C for 1 min, 72°C for 1 min; three cycles of 95°C for 30 s, 52°C for 1 min, 72°C for 1 min; three cycles of 95°C for 30 s, 51°C for 1 min, 72°C for 1 min; 30 cycles of 95°C for 30 s, 50°C for 1 min, 72°C for 1 min; and final extension of 72°C for 10 min).

The PCR amplifications were evaluated by electrophoresis using 1.2% agarose gel stained with GelRed (Biotium, Hayward, CA) and a size standard ladder (100 bp; New England Biolabs). PCR products were purified using exonuclease I (New England Biolabs) and shrimp alkaline phosphatase (USB Products-Affymetrix, Santa Clara, CA), incubating at 37°C for 1 h, followed by 80°C for 20 min. Single sequencing reactions used 1–2 μL of purified PCR product and were performed using the ABI Big Dye Terminator 3.1 cycle sequencing kit (Applied Biosystems, Carlsbad, CA), followed by ethanol cleanup. Labeled fragments were visualized on an ABI 3730 automatic DNA sequencer (Applied Biosystems), and the nucleotide sequences were manually edited with Sequencher 4.9 (Gene Codes Ann Arbor, MI). Sequence data were obtained for all samples across all loci except for *S. eriopus*, which failed to amplify with the PCR markers used for the *40S* and *LiSH* loci. All DNA sequence data (1148 sequences) in this study were deposited in GenBank (app. A).

Sequence Alignment

Sequences for each locus were aligned using MAFFT 7 (Katoh and Standley 2013) and/or aligned manually with Sequencher 4.9. The aligned lengths ranged from 498 bp (*PEX4*) to 1991 bp (*GroES*). Sequence data for different loci were joined using Mesquite 3.2 for concatenated analyses (Maddison and Maddison 2017). Gaps were treated as missing data in all phylogenetic analyses.

The *PSBK/I* chloroplast locus exhibited a 180 bp inversion in the sequences of 16 samples encompassing seven species occurring in the Central American Isthmus (*Zamia cunaria* Dressler & D.W.Stev., *Zamia dressleri* D.W.Stev., *Zamia elegantissima* Schutzman, Vovides & R.S.Adams, *Zamia imperialis* A.S.Taylor, J.L.Haynes & Holzman, *Zamia nana* A.Lindstr., Calonje, D.W.Stev. & A.S.Taylor, *Zamia obliqua* A.Braun, *Zamia pseudoparasitica* J.Yates, and *Zamia stevensonii* A.S.Taylor & Holzman), necessitating the manual realignment of the inverted regions. The inversions could be dealt with by either reverse complementing the inverted sequence region or inserting a 180 base pair gap in the alignment for all sequences that lacked the inversion (Morrison 2009). We chose the latter, as it was not clear whether the single-nucleotide polymorphisms (SNPs) observed resulted from mutations prior to or after the inversion event.

Phylogenetic Analyses

Maximum parsimony and maximum likelihood analyses. Aligned, concatenated sequences for the 10 loci were analyzed using MP performed in PAUP 4.10b (Swofford 2003) for each gene separately and for the concatenated matrix. Heuristic searches were conducted using 1000 random stepwise addition replicates, with the MultTrees option in effect, and saving up to 10 minimum length trees per search for swapping using tree bisection reconnection (TBR) branch swapping. Jackknife analysis was conducted for the concatenated matrix with 37% deletion probability for each character (JK; Farris et al. 1996; 1000

Table 2

Polymerase Chain Reaction (PCR) and Sequencing (SEQ) Primers and Annealing Temperatures

	Forward primer sequence (5′–3′)		Reverse primer sequence (5′–3′)			
Locus ID	Name	Sequence	Name	Sequence	Temperature (°C)	PCR/SEQ
40S	40S_F2	CTGGAAAAGCGAAAGCACAA[b]	40S_R1aa	CATGACTCCAAGATAACAAG	55	PCR/SEQ
	40S_F2bm	TGGAGTTGATAGCTTGGTC	40S_R4m	CAGACGGTTGTGGTGTGT		SEQ
CyAG	CeAG_F7	CCATTTCAGAGTCCAATTCTCAG[a]	AGM_3126r	GCTTAAAGATGTGAGTGCATCTC[a]	60	PCR/SEQ
	CeAG_F8	GCAACAGGAGGCAGGAAAAC[a]	AGM3596_R	CTTAGTGCGAAGAAACTGATTCTC[a]	60	PCR/SEQ
ATG2	ATG2_F1	GTCAATAGCACTGTATGYCA[b]	ATG2_R2	ATAGGACCTTCTTGCAACA[b]	58	PCR/SEQ
GroES	GroES_F1	TYGTGGAAGCTGTGGGGA[b]	GroES_R2b	GTCTCTGGCAATTGAAGAAATG[b]	55/50 (touchdown PCR)	PCR
	GroES_F1b	CTTGGAAGACAGAATTTGGCA	GroES_R2cm2	GGCAATACCMACCTGTCC		SEQ
			GroES_R2cM	CTTCAGGAAATGCCAAAT		SEQ
	GroES_F1c	CCAAGCTGATGATGGTAATTTC[b]	GroES_R2	TACATGGTCWGCTCCTAA[b]	55/50 (touchdown PCR)	PCR
	CyGroES_F1cdd1	ASACATTTCYTGTTAGGGC	CyGroES_r2ab	CCACAAACCTTTCCTATC		SEQ
HTS	HTS_F1aaM	TGTTGGACAGCATGAARA	HTS_R2a	AGTCTCTCTCAACTCAAA[b]	55	PCR/SEQ
LiSH	LisH_F1	CAGGTTGAAGGCAGCATC[b]	LisH_r1m	CAGCCTCCTCTTTTGACA	58	PCR
	LisH_F1c	ATGTGGCCAGATTCATTG	LisH_R7	TTAACATCCGTCATCATACCC		SEQ
	LisH_f1am	TTTGCAGCGGCTTTCTCT	LisH_R4	GTGATTTAGTCATGAAGCAG		SEQ
PEX4	PEX4_F1	TCCAGCTAGCCATGACTGTTC[a]	PEX4_R1	GGTTTTGACCCCTATTCGGTA[b]	55	PCR/SEQ
PMP22	PMP22_F2	CAGCAGGAGATATTGGTGC[b]	PMP22_R3	AGCTWCACACACAAAGAC	60	PCR/SEQ
WRKY4	WRKY4_F2	GGTAGGAGGAAGGAAAAGAAAGT	WRKY4_R1	AATGGCTTTGGGATCATTTG	60	PCR/SEQ
psbK/I	psbK	TTAGCCTTTGTTTGGCAAG[c]	psbI	AGAGTTTGAGAGTAAGCAT[c]	52	PCR/SEQ

Note. All primers without superscripts were developed for this article.

[a] Salas et al. 2013.

[b] Salas et al. 2014.

[c] Lahaye et al. 2008.

replicates with simple stepwise-addition, TBR branch swapping, saving no more than 10 trees per replicate, and retaining only groups with frequencies >50%). A partitioned ML analysis was conducted using IQTREE (Chernomor et al. 2016) as implemented on the CIPRES Science Gateway (Miller et al. 2011) using the automated method selection with ModelFinder (Kalyaanamoorthy et al. 2017), and support was calculated by running 1000 bootstrap replicates.

Time-calibrated species tree. A time-calibrated species tree analysis was performed using the multispecies coalescent model of StarBeast (Heled and Drummond 2010) as implemented in BEAST (ver. 2.4.4; Bouckaert et al. 2014). Samples were assigned to species according to individual taxonomic assessments, resulting in a species tree topology with 77 terminals.

Separate, uncorrelated, log-normal, relaxed-clock models (UCLD) and random starting trees were assigned to each partition, and a birth-death process was applied as branching process prior (or tree prior), as it has shown to be a better fit for cycads than the traditionally used Yule process (Condamine et al. 2015). The following priors were set following Condamine et al. (2015): a uniform prior between 0 and 10 with a starting value of 0.1 for the mean growth rate, a uniform prior between 0 and 1 with a starting value of 0.5 for the relative death rate, an exponential prior with a mean of 0.33 on the standard deviation of the UCLD model, and a uniform prior between 0 and 1 on the mean of the UCLD model. Site models were estimated independently for each partition (table 3) using a Bayesian approach as implemented by the bModelTest package (Bouckaert and Drummond 2017) available in BEAST.

The species tree was calibrated using 95% HPD age estimates obtained from a previously published time divergence analysis of the Cycadales based on six fossil calibrations and the birth-death tree prior (Condamine et al. 2015), as well as from a recently discovered *Zamia* fossil (Erdei et al. 2018). Prior distributions for all calibrated nodes were conservatively set to uniform using the minimum and maximum age bounds outlined below. The age intervals for the tree root node (74.3–147.7 Ma) and the crown node of *Zamia* (9–22.1 Ma), as well as the maximum age bound (84.5 Ma) for the stem node of *Zamia*, were set according to the 95% HPD estimates provided by Condamine et al. (2015). The minimum age bound for the stem group of *Zamia* was constrained to the minimum age estimate (33 Ma) of a fossil cycad leaflet of unknown terrestrial origin recently found preserved in marine sediments of the Gatuncillo Formation in Central Panama, which is assignable to *Zamia* based on cuticular micromorphology (Erdei et al. 2018). The fossil age is considered to be 35–33 Ma based on nannoplankton and foraminiferal biostratigraphy, and the minimum age estimate (33 Ma) was used to constrain the minimum age bound for the stem group of *Zamia*. This age is comparable to the lower bound of the 95% HPD estimate (34.2 Ma) obtained by Condamine et al. (2015).

Table 3

Site Models with Highest Posterior Support Selected by bModelTest

Locus ID	Posterior support	Model (r_{ac} r_{ag} r_{at} r_{cg} r_{ct} r_{gt})
40S	33.21%	121,231
CyAG	31.65%	123,121
ATG2	10.84%	121,321
GroES	20.53%	121,343
HTS	17.69%	121,321
LiSH	25.56%	123,451
PEX4	10.26%	121,323
PMP22	11.52%	123,221
psbK/I	18.63%	123,324
WRKY4	13.91%	121,231

Two independent runs of 750 million Markov chain Monte Carlo (MCMC) iterations were conducted, sampling every 2500 iterations and preceded by a 100 million iteration burn-in period. Log and tree files were combined using Logcombiner (ver. 2.4.4, included in BEAST), resulting in 600,000 trees. The log output was evaluated using Tracer (ver. 1.6; Rambaut et al. 2014), and a maximum clade credibility (MCC) tree was created from these trees using TreeAnnotator (ver. 2.4.4, included in BEAST) and visualized using Figtree (ver. 1.4.3; Rambaut 2012). The MCC tree topology recovered was used for the diversification, biogeographic, and ancestral character state reconstruction analyses presented here.

Diversification Analyses

Diversification rates were estimated per-million-year interval spanning 10–0 Ma for the crown node of *Zamia* as well as several major clades within the genus using the dates derived from the time-calibrated species tree. The rates were obtained using Foote's (Foote 2000) equation for per-capita origination rates as modified to apply to molecular tree lineages by Nagalingum et al. (2011). We examined changes in diversification rates for each of the major clades using the APE package for R (Paradis et al. 2004) to calculate the γ statistic (Pybus and Harvey 2000) from the branching times in the time-calibrated species tree. The γ statistic is a metric of the distribution of speciation times in molecular phylogenies, with negative values indicating early diversification and positive values indicating late branching. A Monte Carlo constant rates (MCCR) test was conducted to determine whether the distribution of diversification rates significantly differed from a constant rate ($P < 0.05$). The MCCR test simulates a distribution for the γ statistic by simulating trees that take into account the incomplete lineage sampling of the observed tree and providing a critical value for rejecting a constant diversification rate. The MCCR test was conducted using the LASER package in R (Rabosky 2006) by simulating 10,000 trees under a pure birth model. Lineage through time (LTT) plots were prepared using the time-calibrated species tree using the APE package in R. We examined the stem and crown nodes of *Zamia* as well as several major clades within the genus.

Net diversification rates were calculated according to Magallon and Sanderson (2001) using the package Geiger (Harmon et al. 2008) as implemented in R. The method requires the input of the extinction rate as a fraction of the speciation rate (e), but since the extinction rate cannot be reliably estimated, we followed previous recommendations (Magallon and Sanderson 2001; Crisp and Cook 2011) to provide net diversification rate estimates based on several values ranging from low ($e = 0$) to high ($e = 0.9$).

The Comet model (May et al. 2016) from the R package TESS (Höhna et al. 2016) was used to test for shifts in speciation or extinction rates as well as for the signature of mass extinction in the crown node of *Zamia*. We selected a single prior for

the diversification shift to represent a slowdown after the origin of the crown of *Zamia*. For the mass extinction priors, we chose a prior with three events, representing (1) the first appearance of polar ice caps during the Late Miocene ca. 7 Ma, (2) the Messinian glaciation (6.26–5.5 Ma), and (3) the start of the Pleistocene glaciations (2.58 Ma; Hodell et al. 2001; Herbert et al. 2016). The survival rate prior was set to 0.05, representing a major extinction event.

We used BAMM 2.5.0 (Rabosky 2014) to test evolutionary rate heterogeneity in the topology of the crown node of *Zamia* using the default priors and settings recommended by the developers.

Ancestral Character State Reconstruction

We used Mesquite 3.02 (Maddison and Maddison 2017) to study the evolution of four morphological characters on the calibrated species tree by performing ancestral character state reconstruction using parsimony. The morphological characters used were presence of prickles on the petiole, prominence of teeth along leaflet margin, prominence of leaflet veins, and arborescence (table 4). These characters were selected because they are considered informative and are commonly used to diagnose different species within the genus.

Zonneveld and Lindström (2016) examined genome sizes of most *Zamia* species and inferred a Mexican center of origin for *Zamia* with a migration south to South America based on increasing DNA content in the southernmost species. Furthermore, they proposed Mega-Mexico, Caribbean Island, and South American biogeographic groupings based on genome size, with several Central American species falling into different groupings based on purported ancient hybridizations. We examined these inferences by examining the evolution of genome size using the species tree topology. For this purpose, we used the function contMap from the phytools R package (Revell 2012) to map the haploid genome sizes (1C) compiled by Zonneveld and Lindström (2016) onto a pruned phylogeny for the crown group of *Zamia*. We used the function phylosig to compute the phylogenetic signal using Pagel's λ. This statistic reflects the similarity of the observed trait distribution to the result of a passive Brownian motion process, with a perfect fit indicated by a lambda of 1. We conducted this analysis to test whether genome size passively reflects the relationships between species and clades instead of being related to a north to south increase.

Biogeographic Analyses

The historical biogeography of *Zamia* was inferred using a statistical dispersal-vicariance analysis (S-DIVA; Yu et al. 2010) as implemented in RASP 3.2 (Yu et al. 2015). The MCC tree resulting from the time-calibrated species tree analysis was selected as the condensed tree, and the 600,000 individual post-burn-in trees obtained from the analysis were resampled to a more manageable 14,000 trees using Logcombiner 2.4.4. Of these, 100 were randomly selected in RASP for the analysis. Areas coded for the analysis include the following: A = Caribbean, B = Mesoamerica, C = Isthmus, D = South America, and E = South Africa. The maximum number of ancestral areas at each node was constrained to four, and the estimated probabilities of the ancestral areas were visualized on the condensed tree.

We also reconstructed the historical biogeography of *Zamia* using BioGeoBEARS (Matzke 2013). Analyses were conducted using the dispersal-extinction-cladogenesis (DEC) and DIVA-like models, as well as variants of these models with the jump parameter (DEC+J and DIVA+J). All analyses were nonstratified and with equal probability of transition between areas. Ancestral area number occupancy was limited to two areas at the time.

Data Availability

The following data used in or resulting from the analyses in this article have been uploaded and are available on the FigShare public file repository at https://figshare.com/s/34b73962882c8adb0c73. They include (1) the partitioned sequence alignment used for all phylogenetic analyses, (2) the results of the BioGeoBEARS biogeographical analyses, and (3) the following phylogenetic trees: time-calibrated MCC species trees as well as individual locus trees resulting from the StarBEAST analysis, trees resulting on concatenated matrix and partitioned ML analyses, and trees based on MP analyses of concatenated matrix and individual loci.

Results

Single Locus and Concatenated Matrix Sequence Characteristics

Single locus MP analyses generally yielded poorly resolved consensus trees (see data availability), indicating that the incongruence between them is most likely soft incongruence because of the weak phylogenetic information of most individual gene trees, rather than hard incongruence, which is due to significantly conflicting topologies (Wendel and Doyle 1998). The range of parsimony informative characters (table 5) ranged from 29 (*PEX4*) to 127 (*GroES*), or by percentage, from 5.1% (*LiSH*) to 10.2% (*ATG2*). Consistency indexes (CI) were above 0.82, and retention indexes (RI) were above 0.89 for all examined to-

Table 4

Characters and Character States for Ancestral Character State Reconstruction Using Parsimony

Character	Character states
Presence of prickles on petiole	0 absent; 1 present
Prominence of teeth on leaflet margin	0 prominent; 1 not prominent;
Prominence of leaflet veins	0 prominent; 1 not prominent; 2 variable
Arborescence	0 subterranean stem; 1 arborescent stem

Table 5

Sequence Characteristics of 10 Loci and Concatenated Matrix (Supermatrix) across 113 Samples of *Zamia*, One Sample of *Microcycas*, and One Sample of *Stangeria*

Locus ID	Alignment length	Parsimony informative characters	% Parsimony informative characters	No. trees found	Tree length	Consistency index	Retention index	Homoplasy index
40S (excluding *Stangeria*)	1096	91	8.3	7970	257	.821	.958	.179
CyAG	1289	111	8.6	8950	418	.859	.913	.141
ATG2	696	71	10.2	8750	188	.888	.923	.112
GroES	1991	127	6.4	4190	450	.871	.947	.129
HTS	820	63	7.7	9400	219	.877	.949	.123
LiSH (excluding *Stangeria*)	1263	64	5.1	7200	231	.853	.965	.147
PEX4	498	29	5.8	3750	98	.969	.977	.031
PMP22	574	39	6.8	9750	125	.816	.956	.184
WRKY4	791	48	6.1	6220	168	.982	.988	.018
PsbK/I	980	52	5.3	9680	167	.844	.885	.156
Supermatrix	9998	695	7.0	1820	2776	.728	.869	.272

pologies (Wendel and Doyle 1998). The concatenated matrix consisted of 9998 characters, 7% of which were parsimony informative, and the MP analysis yielded a total of 1820 equally parsimonious trees (tree length = 2775, CI = 0.728; homoplasy index [HI] = 0.272; RI = 0.869).

Major Clades Recovered

The MP concatenated analysis, ML partitioned analysis, and Bayesian inference (BI) species tree approach recovered the genus *Zamia* as monophyletic and sister to *Microcycas*. All analyses recovered the same broad topology consisting of the following geographically delimited major clades (fig. 3): (1) Caribbean clade, consisting mostly of Caribbean Island species (a single species, *Zamia integrifolia*, also reaches Florida), which is sister to the rest of the genus consisting of primarily of mainland American species; (2) Fischeri clade, consisting of three Mexican endemic species and is itself sister to the rest of the genus excluding the Caribbean clade; (3) Mesoamerica clade, including all other species occurring in Mesoamerica to the exclusion of the Fischeri clade and *Zamia soconuscensis*; (4) Isthmus clade, consisting primarily of Panamanian and Costa Rican species; and (5) South America clade, consisting primarily of South American endemic species. The latter two clades are sister to each other and together form the most species-rich and morphologically diverse clade in the genus, referred to here as the Central-meridional clade. All the above clades were strongly supported by all analyses except for the Mesoamerica clade, which was recovered by all analyses, albeit with poor support (MP = 57.8%, ML = 50%, BI = 0.63).

Maximum Parsimony, Maximum Likelihood, and Species Tree Inference Analyses

Although all phylogenetic methods resolved the same broad topologies and recovered the same major clades (fig. 3), the species tree analysis recovered several relationships more congruent with morphological similarities and/or geographic proximity than the other two analyses and will therefore be used in this article to discuss phylogenetic relationships, node age estimates, and biogeographic patterns within the genus *Zamia*. The MP (fig. B1; figs. B1, B2, C1, C2, D1–D5 are available online) and ML (fig. B2) trees are presented in the online figures and will be referred to primarily in the context of topological and node support congruency with the MCC species tree topology (fig. 4).

Time-Calibrated Species Tree

Single-locus MCC trees produced by StarBeast analysis generally yielded poorly resolved trees (see data availability) compared with the species tree topology (fig. 4). The effective sample size (ESS) scores from the time-calibrated species tree analysis were all above 200, indicating good levels of convergence of the MCMC. The mean stem age of *Zamia* was calculated at 68.28 Ma (95% HPD 51.0–84.5) and the crown age at 9.54 Ma (95% HPD 9.0–10.62; fig. 5; table 6). The crown node that includes the Mainland *Zamia* clade is the oldest within the genus, with a mean age of 5.97 Ma (95% HPD 3.9–8.2). The Caribbean clade, despite being sister to the rest of the genus, has the youngest crown age—1.19 Ma (95% HPD 0.61–1.86)—of the major clades. The Fischeri clade, despite consisting of only three species, is relatively old, with a crown age of 2.59 Ma (95% HPD 0.75–4.62). The Mesoamerica clade, with a crown age of 3.9 Ma (95% HPD 2.54–5.34) is of comparable age to the Central-meridional clade, which is 3.8 Ma (95% HPD 2.49–5.17). Within the Central-meridional clade, the South America clade, with a crown age clade of 2.62 Ma (95% HPD 1.71–3.56), is slightly older than the Isthmus clade, which is 2.35 Ma (95% HPD 1.43–3.32).

Diversification Analyses

Net diversification rates. Net diversification rates were highest when lower extinction rate (ϵ) values were used in the calculations (table 8). The net diversification rate for the crown of *Zamia* ranged from 0.22 to 0.39. Among the major clades examined, using ϵ values of 0 and 0.7, the Caribbean clade had the highest diversification rates (1.26, 1.26, 0.88), followed by the South America clade (1.04, 1.03, 0.81) and the Isthmus clade (0.88, 0.65, 0.37). The lowest diversification rates were found in the species-poor Fischeri clade (0.16, 0.10, 0.05), followed by the Mesoamerica clade (0.60, 0.46, 0.27). In the analysis

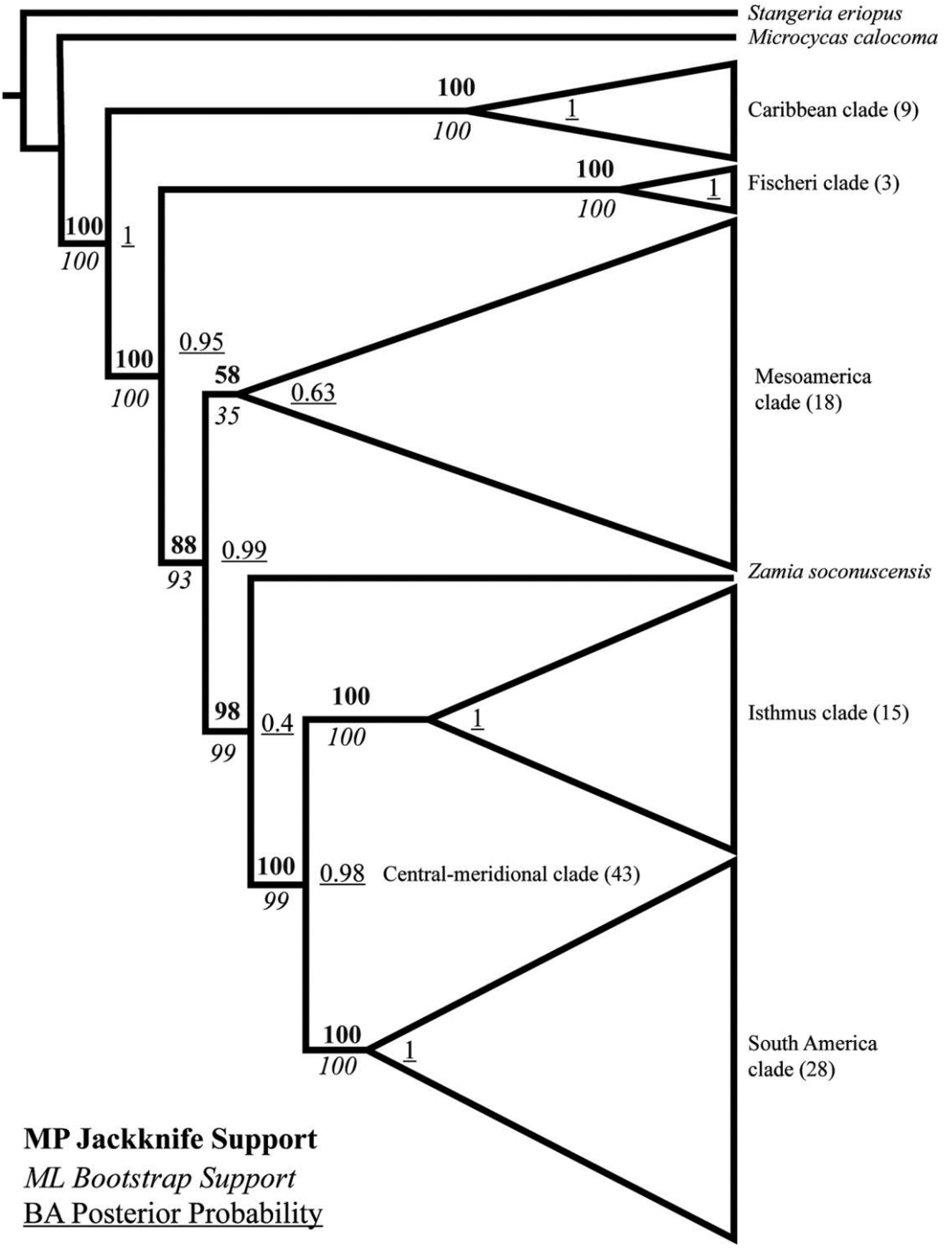

Fig. 3 Broadly congruent tree topology obtained from maximum parsimony (MP; PAUP), maximum likelihood (ML; RAXML), and Bayesian species tree (BEAST) analyses (BA) of nine single-copy nuclear gene loci and one plastid locus. All methods resolved the same major clades and relationships between them. Underlined numbers to the right of nodes are posterior probabilities from the BA, numbers below branches in italics are bootstrap support values for ML, and numbers above branches in boldface are jackknife support values for the MP analysis. Numbers in parentheses next to clade names represent the number of taxa included in these clades.

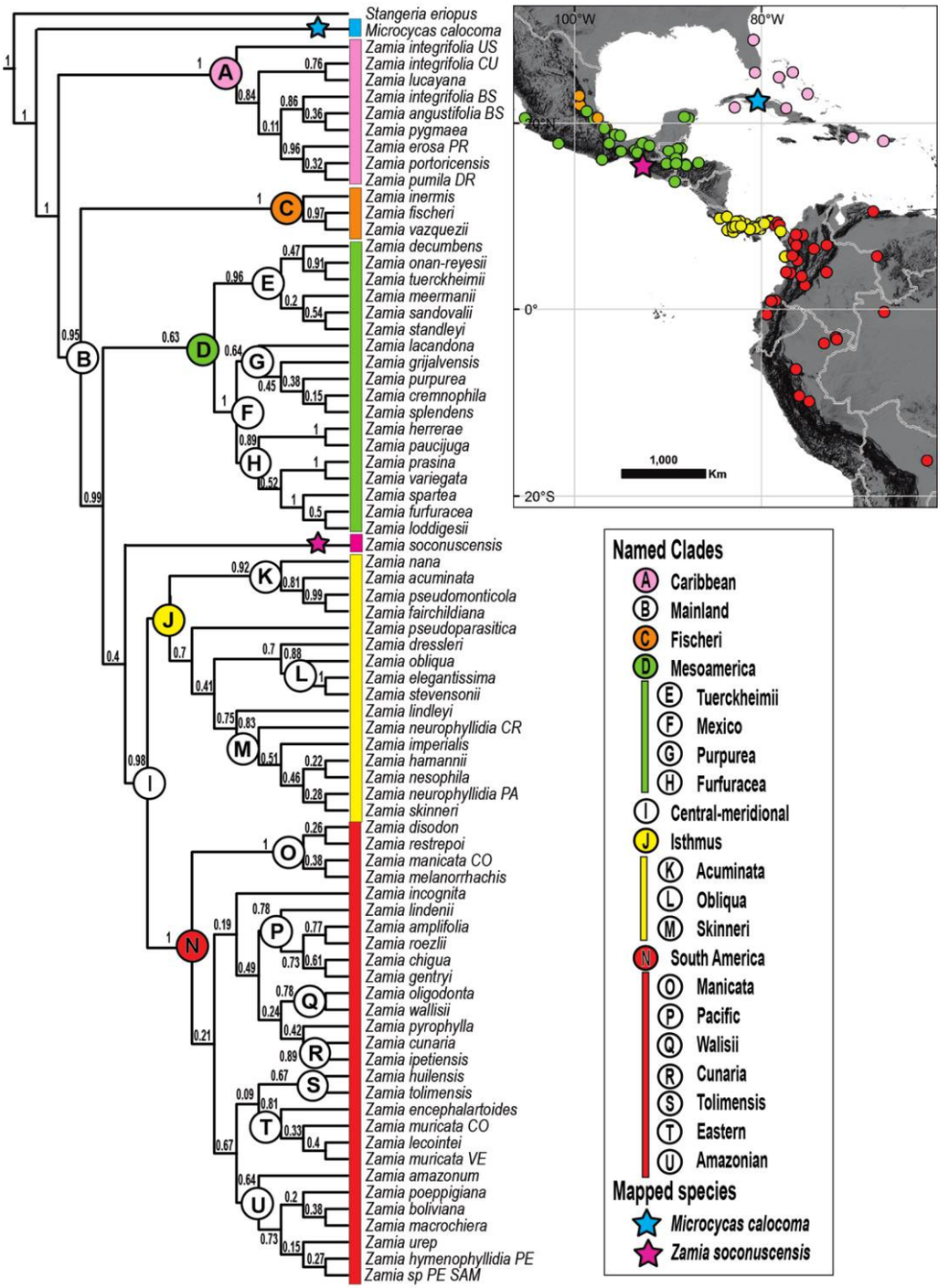

Fig. 4 Maximum clade credibility species tree cladogram obtained from analysis in StarBeast using nine single-copy nuclear genes and one plastid locus. Posterior probabilities displayed above branches. Circles at nodes are labeled with letter codes identifying clade names with major clades color coded. Inset map shows the geographic provenance of the samples used in this study, color coded by major clade membership.

using $\varepsilon = 0.9$, the diversification rate was slightly higher for the South America clade than the Caribbean clade. However, ε values of 0.9 are exceptionally high (Magallon and Sanderson 2001) and may be unrealistic for such a short time frame, so the results using $\varepsilon = 0.9$ should be interpreted with caution.

Per-million-year diversification and diversification rate heterogeneity. Most diversification above the crown node of *Zamia* occurred in the Pliocene and Pleistocene epochs (figs. 6, D1), with only the split between the Caribbean and Mainland clade and between the Fischeri clade and the rest of the Mainland

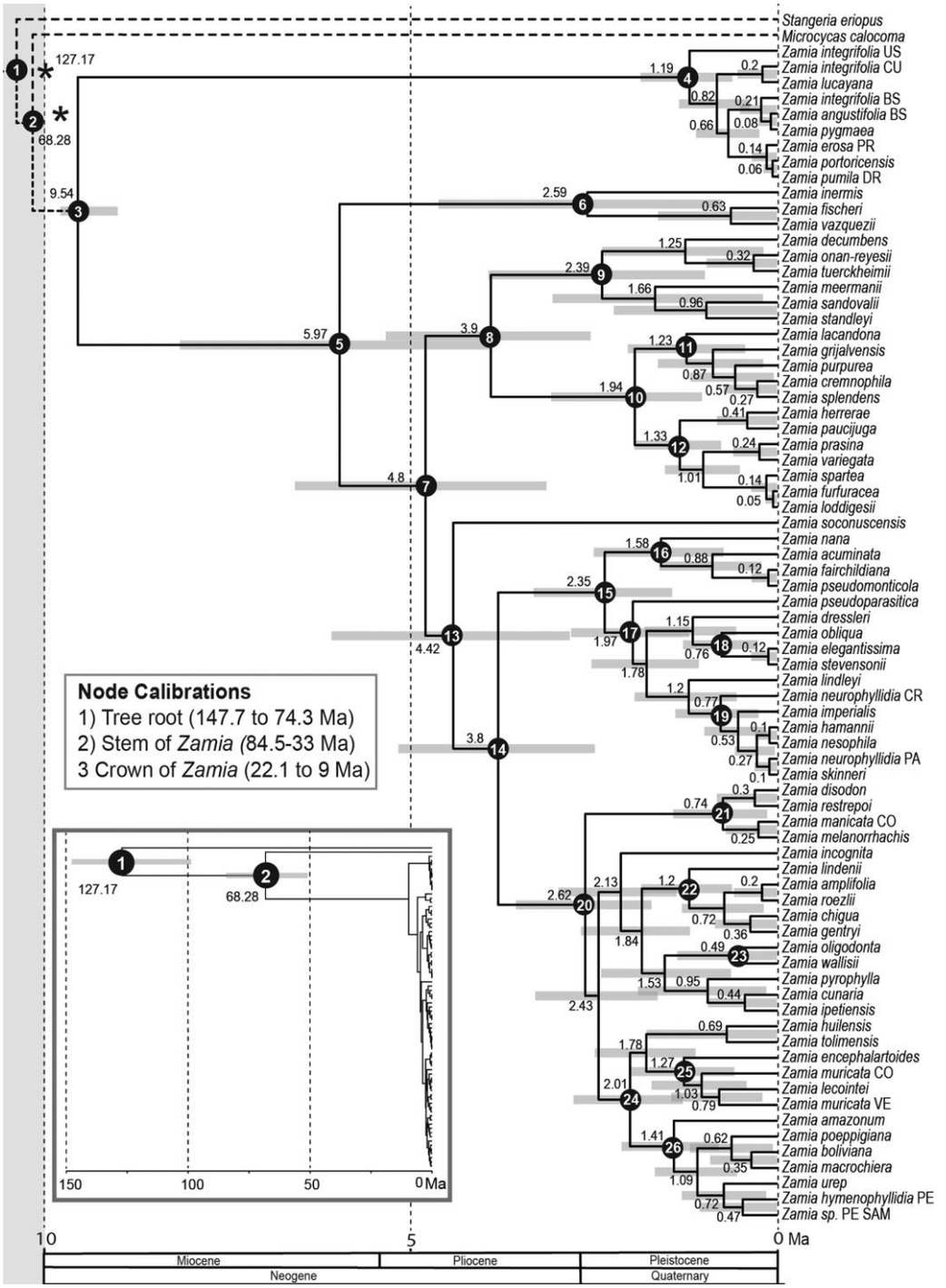

Fig. 5 Maximum clade credibility species tree chronogram obtained from analysis in StarBeast using nine single-copy nuclear genes and one plastid locus. Numbers on branches are mean estimated ages of clades (Ma). The gray bars represent the 95% highest posterior density (HPD) indexes. The numbered nodes are referenced in table 6 with 95% HPD indexes for stem and crown nodes. Nodes 1 and 2 (connected to dotted branches) are out of range of the main figure; inset map shows their true positions and ages. Holocene epoch not shown. Posterior probability support values for all nodes reported in figure 4.

Table 6

Selected Mean Clade Ages in Millions of Years Ago and Their 95% Highest Posterior Density (HPD) Intervals from Dated Species Tree Analysis with StarBeast of the Genus *Zamia* (Fig. 4)

	Stem		Crown	
Node	Mean	95% HPD	Mean	95% HPD
1	na	na	127.17	98.74–147.7
2	127.17	98.74–147.7	68.28	50.99–84.5
3	68.28	50.99–84.5	9.54	9–10.62
4	9.54	9–10.62	1.19	.61–1.86
5	9.54	9–10.62	5.97	3.92–8.15
6	5.97	3.92–8.15	2.59	.75–4.62
7	5.97	3.92–8.15	4.8	3.15–6.58
8	4.8	3.15–6.58	3.9	2.54–5.34
9	3.9	2.54–5.34	2.39	.99–3.94
10	3.9	2.54–5.34	1.94	1.02–3.08
11	1.94	1.02–3.08	1.23	.43–2.04
12	1.94	1.02–3.08	1.33	.76–1.95
13	4.8	3.15–6.58	4.42	2.83–6.08
14	4.42	2.83–6.08	3.8	2.49–5.17
15	3.8	2.49–5.17	2.35	1.43–3.32
16	2.35	1.43–3.32	1.58	.73–2.5
17	2.35	1.43–3.32	1.97	1.2–2.81
18	1.15	.55–1.81	.76	.26–1.28
19	1.2	.55–1.94	.77	.25–1.38
20	3.8	2.49–5.17	2.62	1.71–3.56
21	2.62	1.71–3.56	.74	.14–1.41
22	1.84	1.19–2.67	1.2	.61–1.85
23	1.53	.63–2.4	.49	0–1.36
24	2.43	1.63–3.3	2.01	1.29–2.77
25	1.78	1.11–2.48	1.27	.58–2.01
26	2.01	1.29–2.77	1.41	.8–2.12

Note. na = not applicable.

clade occurring in the Miocene. The highest per-million-year diversification rates were found in the Caribbean clade followed by the South America clade (fig. 6; table 9), which were the two clades that also had the highest net diversification rates. Among the major *Zamia* clades, the MCCR tests only found diversification rates differing significantly from constant ($P < 0.05$) in the South America clade. In this case, the negative γ statistic indicated rapid, early diversification of the South America clade followed by a decrease in diversification rate over time. Similarly, the BAMM analysis did not uncover shifts in diversification rates across the tree. Finally, the TESS analysis showed no evidence of shifts in extinction or diversification rates and only marginal evidence of mass extinctions at around 6 and 2.5 Ma (fig. D2).

Ancestral Character State Reconstruction

Morphological characters. All four morphological traits examined exhibited homoplasy, and the ancestral states recovered include subterranean stems, smooth petioles, entire leaflet margins, and leaflets without prominent veins (figs. D1–D4). Arborescence (fig. D1) is absent in the Caribbean clade and rare in the Mesoamerica clade, where it is restricted to only three species. The ancestral state for the Central-meridional clade is ambiguous, leading to an ancestral state of arborescence for the Isthmus clade and subterranean stems for the South America clade. Arborescence is most prevalent in the Isthmus clade, with only two species possessing subterranean stems. Within the South America clade, arborescence seems to have evolved separately four times. Regarding petiole armature, unarmed petioles are universal within the Caribbean clade but extremely rare among mainland species (fig. D2). Both leaflet margin dentation (fig. D3) and leaf venation prominence (fig. D4) are extremely homoplastic characters that appear to have evolved independently multiple times within the genus and may be of limited use as diagnostic characters.

Genome sizes in Zamia. We recovered a strong phylogenetic signal on the evolution of genome size within the crown group of *Zamia* (Pagel's $\lambda = 0.9721436$), with both genome expansion and contraction occurring within different lineages (fig. D5).

Biogeographic Analyses

Historical biogeography of Zamia. Optimization of ancestral areas on the species tree using S-DIVA (fig. 7) required six dispersal and five vicariance events (table 7), with most speciation events occurring within geographical areas. Dispersal events occurred from the Mesoamerica (B) region to the Isthmus (C) and South America (D) regions, from the Isthmus to the South America region, and from South America to the Isthmus region.

The crown node of *Zamia* + *Microcycas* (node 152, probability of ancestral range at node, $P = 0.52$) is optimized in two areas, one being the Caribbean (A) region, the other being a composite area including the Caribbean (A) and Mesoamerican (B) regions, with a dispersal event from the composite area to the Caribbean region. The crown node of *Zamia* (151, $P = 1$) is optimized in a composite area consisting of the Caribbean (A) and Mesoamerica (B) regions with a vicariance between these two regions separating the Caribbean clade from the rest of the genus on the American mainland. The Caribbean clade is ancestrally optimized in the Caribbean (A) region with no events hypothesized (85, $P = 1$), and stasis within all inner nodes (78–84, all with $P = 1$). The crown node of the clade including all mainland zamias (150, $P = 0.63$) is optimized in the Mesoamerican region (B) with no events hypothesized. The crown node of the Fischeri clade is optimized to the Mesoamerica region (87, $P = 1$) with no events hypothesized. The clade including all *Zamia* except the Caribbean and Fischeri clade (149, $P = 0.21$) has a poorly supported optimization among four areas, with the highest support value found for the Mesoamerican region (B, 62.6%). The other three areas were all composite areas that included the Mesoamerica region. Two dispersal events are hypothesized from the Mesoamerica region to the Isthmus and South America regions. The Mesoamerica clade (104, $P = 1$) is optimized in the Mesoamerican region with high probability ($P = 1$), no events hypothesized and stasis within all inner nodes (88–103, all with $P = 1$). The node that includes *Zamia soconuscensis* as sister to the Central-meridional clade has a poorly supported optimization (148, $P = 0.34$) consisting of three composite areas, all of which include the Mesoamerican region and vicariance between Mesoamerica and a composite area consisting of the Isthmus and South America regions.

The split of the Central-meridional clade (147, $P = 0.98$) into the Isthmus and South America clades was attributed to a vicariance event occurring 3.8 Ma (95% HPD 2.49–5.17)

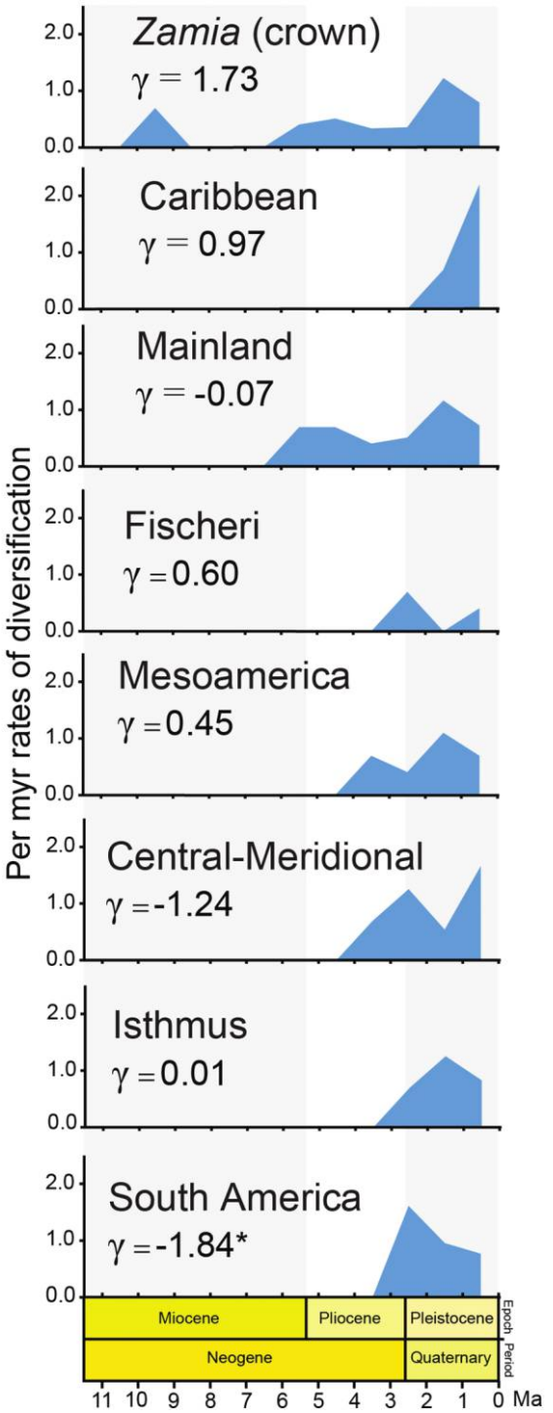

Fig. 6 Per-million-year diversification rates and γ values for major *Zamia* clades. Only the γ value for the South America clade (asterisk) was significant, indicating that diversification was initially high and that it decreased over time. The γ value for all other clades was not significant, indicating a constant diversification rate.

from a well-supported ($P = 0.98$) ancestral composite area including the Central American Isthmus and South America. The Isthmus clade (146, $P = 1$) is optimized in that region with no events hypothesized. Stasis is maintained in all inner nodes except the crown node including *Zamia obliqua*, *Zamia stevensonii*, and *Zamia elegantissima*. This node is optimized for the Isthmus (C) region with one dispersal event of *Z. obliqua* into the South America (D) region. The South America clade (131, $P = 0.98$) is mostly optimized for that region (D, 97.5%) with no events hypothesized and all but a few inner nodes in stasis. Of note is the clade (110, $P = 1$) that includes *Zamia pyrophylla* Calonje, D.W.Stev. & A.Lindstr., *Zamia cunaria*, and *Zamia ipetiensis* D.W.Stev., which is optimized to a composite area including the Isthmus (C) and South America (D) regions with one vicariance event between these two regions.

The ancestral areas recovered for nodes using the DIVA and DEC models in BioGeoBEARS and the S-DIVA model in RASP were identical and differed only slightly in their area probabilities. Implementing the jump parameter, a jump between Mexico and South America (in the DEC+J) or Mexico and Central America (in the DIVA+J) at the base of the Central-meridional clade is favored. However, given the issue that recently emerged with the jump parameter estimation (Ree and Sanmartín 2018), the results of the DEC+J and DIVA+J must be viewed with caution. As the BioGeoBEARS analyses recovered the same ancestral areas as the S-DIVA analysis, albeit with slightly different area probabilities, we will limit our discussion of the historical biogeography of *Zamia* to the results of the RASP S-DIVA analysis. The BioGeoBEARS analyses are available in the FigShare file repository (see data availability).

Discussion

Utility of psbK/I *for Barcoding and Phylogenetic Analyses*

Despite the high rate of amplification success across all cycad genera and a high number of diagnostic sites for DNA barcoding demonstrated for *psbK/I* (Nicolalde-Morejón et al. 2011), its utility for barcoding and phylogenetic inference may be limited by the fact that sizable inversions are present in several taxa. If the inversions are not detected or dealt with during multiple sequence alignment, they could prove problematic because they would result in multiple false-positive SNPs. For example, the unusually high number of plant barcoding diagnostic sites reported for *Zamia pseudoparasitica* by (Nicolalde-Morejón et al. 2010) appears to be due to an inversion present in this species that was neither reverse complemented nor staggered during the alignment process. A comparable situation has also been found in the chloroplast barcoding candidate locus *trnH-psbA*, where frequent inversions in multiple angiosperm lineages present a challenge to the gene's utility as a plant barcoding region (Whitlock et al. 2010).

Phylogenetic Relationships and Major Clades within Zamia

Below we consider the phylogenetic relationships within *Zamia*, providing brief descriptions of the major clades recovered in our analyses as well as for some notable subclades that we define for the first time below. Informal names are provided for these monophyletic groups for the purposes of discussion clarity (fig. 4).

Monophyly of Zamia. The monophyly of *Zamia* was strongly supported (fig. 4, node A; BI/MP/ML = 1/100/100) and its sister relationship to *Microcycas* was recovered in all anal-

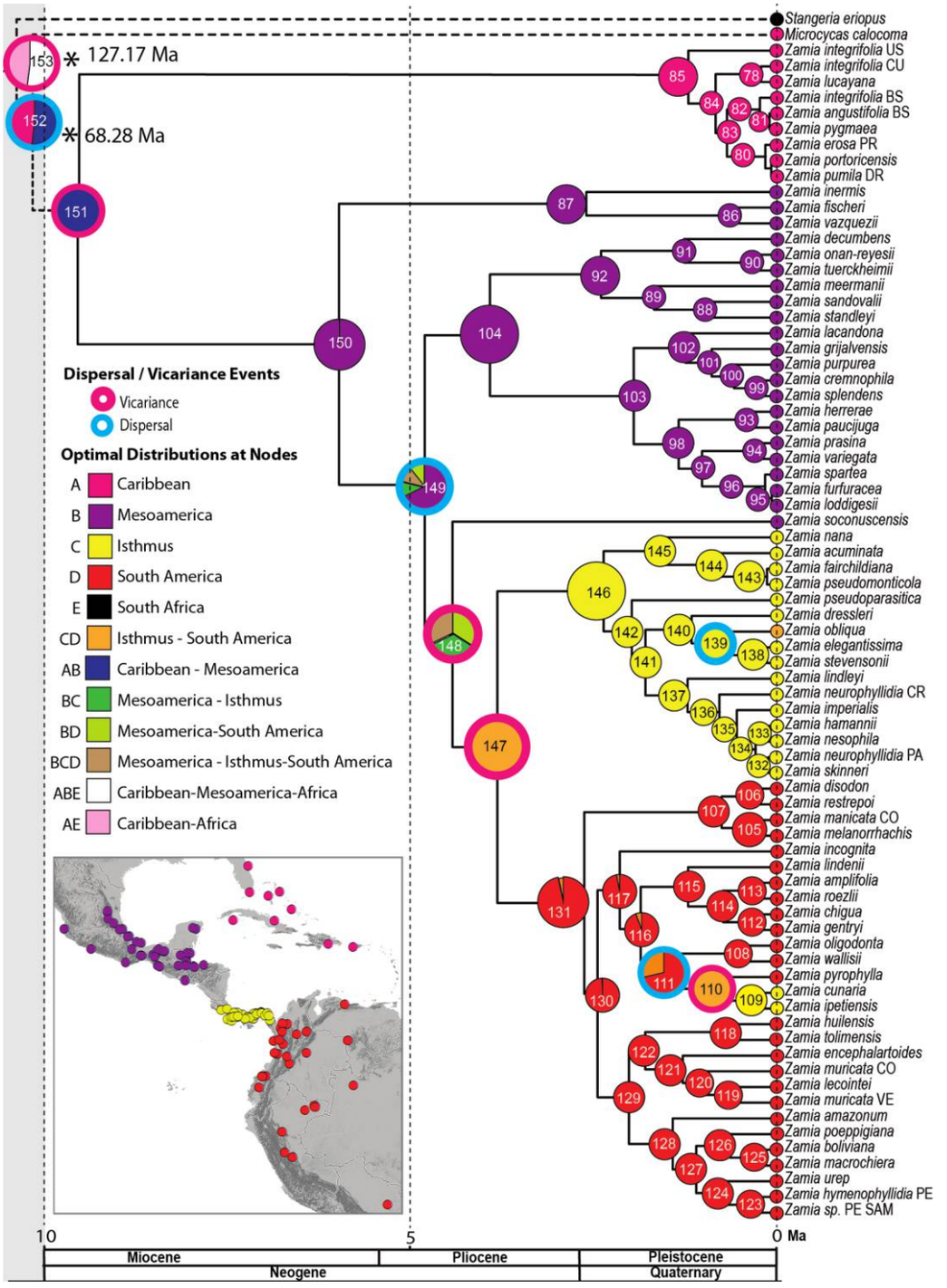

Fig. 7 Historical biogeography of *Zamia* inferred using a statistical dispersal-vicariance analysis as implemented in RASP using the maximum clade credibility chronogram tree shown in figure 4. The proportions of colors in circles represent possible ancestral geographic ranges at each node, and the rings around the circles represent dispersal and/or vicariance events. The two basalmost nodes are out of scale; their mean ages are indicated next to the asterisks. Inset map shows the geographic distribution of the *Zamia* samples color coded by their area assignations.

yses. *Zamia* consists of two sister clades: the Caribbean clade, consisting primarily of Caribbean Island species, and the Mainland clade, which largely consists of mainland American species.

Caribbean clade. The Caribbean clade (fig. 4, node A; BI/MP/ML = 1/100/100) consists of nine species with subterranean stems, unarmed petioles, and the same 2n=16 chromosome number (Olson and Gorelick 2011). The group is primarily distributed on several islands in the Greater Antilles and Bahama Archipelago, with a single mainland species restricted mostly to Florida, albeit with a few historical collections in ex-

Table 7

Nodes with Dispersal and Vicariance Events from Reconstruct Ancestral State in Phylogenies (RASP) Dispersal-Extinction-Cladogenesis Analysis

Node	Ancestral area	Child taxa	Child nodes	Event(s)	RASP route	Probability
110	CD 100.00	*Zamia pyrophylla*	Node109: C 100.00	Vicariance: 1	CD->D|C	1
111	D 80.43 CD 19.57		Node110: CD 100.00; node108: D 100.00	Dispersal: 1	D->D^D->CD^D->CD|D	.8043
139	C 100.00	*Zamia obliqua*	Node138: C 100.00	Dispersal: 1	C->C^C->CD^C->CD|C	1
147	CD 100.00		Node146: C 100.00; node131: D 97.50 CD 2.50	Vicariance: 1	CD->C|D	.975
148	BCD 33.74 BD 33.74 BC 32.52	*Zamia soconuscensis*	Node147: CD 100.00	Vicariance: 1	BCD->B|CD	.3374
149	B 62.63 BCD 12.79 BD 12.46 BC 12.12		Node148: BCD 33.74 BD 33.74 BC 32.52; node104: B 100.00	Dispersal: 2	B->B^B->BCD^B->BCD|B	.2113
151	AB 100.00		Node150: B 100.00; node85: A 100.00	Vicariance: 1	AB->B|A	1
152	AB 52.00 A 48.00	*Microcycas calocoma*	Node151: AB 100.00	Dispersal: 1	AB->AB^A->A|AB	.52
153	ABE 52.00 AE 48.00	*Stangeria eriopus*	Node152: AB 52.00 A 48.00	Vicariance: 1	ABE->E|AB	.2704

treme southeast Georgia (Duncan 1979). Caribbean zamias are universally accepted as a distinct lineage (e.g., Eckenwalder 1980*a*; Stevenson 1987; Sabato 1990), yet their current classification (e.g., Stevenson 1987; González-Géigel 2003; Osborne et al. 2012) remains controversial. This classification is primarily based on a historic overreliance on vegetative morphological characters, especially leaflet macromorphology, for species delimitations. Consequently, populations exhibiting similar leaflet morphologies are currently considered conspecific (González-Géigel 2003) despite sometimes occurring on geographically distant islands that in many cases were never connected by land. This scenario would require multiple occurrences of long-distance dispersal over the Caribbean Sea. An alternative explanation is that some of these morphotypes may have evolved independently multiple times within the clade. Recent genetic studies have begun to address this question and provided further insight into the genetic relationships within this group (Meerow 2007; Meerow et al. 2012; Salas-Leiva et al. 2017; Meerow et al. 2018). Ongoing systematics research should help clarify the currently controversial taxonomy of Caribbean zamias in the near future.

Mainland clade. The Mainland clade (fig. 4, node B, BI/MP/ML = 1/100/100) is sister to the Caribbean clade and consists chiefly of species occurring on the American mainland, with only a few species also occurring on nearshore continental islands (e.g., *Zamia hamannii* A.S.Taylor, J.L.Haynes & Holzman). It is the most species-rich group in *Zamia* (90% of species) and has a broad geographic range that extends from Mexico to Bolivia. It consists of multiple geographically defined clades discussed below.

Fischeri clade. The Fischeri clade (fig. 4, node C, BI/MP/ML = 1/100/100) is sister to all remaining mainland species and consists of three species occurring in northeastern Mexico. *Zamia fischeri* Miq. and *Zamia vazquezii* D.W.Stev., Sabato & De Luca are morphologically very similar, with the latter segregated from the former based on differences in leaf size, leaflet shape and texture, and differing chromosome counts (Stevenson et al. 1998). Our analyses confirm that the two species form a monophyletic group, and we report for the first time this group's sister relationship to *Zamia inermis* Vovides, J.D.Rees & Vázq.Torres. All three species occur in relative geographic proximity and have unarmed or sparsely armed petioles and stems that are subterranean or very short. In addition, *Z. inermis* shares the same chromosome count (2n = 16) as *Z. fischeri* (Vovides 1983; Stevenson et al. 1998) and has a reproductive phenology similar to that of *Z. vazquezii* (Griffith et al. 2012).

Mesoamerica clade. This group (fig. 4, node D) of 18 species is restricted to the Mesoamerican dominion (sensu Morrone 2014), which it shares with *Zamia soconuscensis* and the three Fischeri clade species. The clade was recovered in all analyses, albeit with low support (below 70%). It is divided into the sister Tuerckheimii and Mexico subclades. The Tuerckheimii subclade (fig. 4, node E), recovered only in the species tree analysis with high support (BI = 0.96), is a group consisting of six species endemic to Guatemala, Honduras, and Belize. The Mexico subclade (fig. 4, node B; BI/MP/ML = 1/98.4/100) consists of mostly Mexican endemic species with subterranean stems, armed petioles, and dentate leaflet margins. This group is further divided into sister Purpurea and Furfuracea subclades. Although the Purpurea subclade (fig. 4, node G) was only poorly supported in the species tree analysis (BI = 0.64), its constituent species have been recognized as morphologically distinct by several authors (e.g., Schutzman 1984; Schutzman and Vovides 1998; Pérez-Farrera et al. 2012), albeit always with the inclusion of *Zamia standleyi* Schutzman, which in our results was resolved as deeply embedded within the Tuerckheimii subclade (fig. 4, node E). *Zamia katzeriana* (Regel) E.Rettig, considered by Pérez-Farrera et al. (2016) to be a species of hybrid origin, may belong in this group (see Nicolalde-Morejón et al. 2008) but was not included in our sampling. The Furfuracea clade (fig. 4, node H; BI/MP/ML = 0.89/52.4/67) consists of subterranean-stemmed species, most of which are endemic to Mexico with a few species extending into neighboring countries.

Phylogenetic placement of Zamia soconuscensis. Surprisingly, the Mexican species *Zamia soconuscensis* was recovered as sister to all species from the Central American Isthmus region and South America and does not appear to be closely related to other Mesoamerican species. This inclusive clade was strongly supported in the MP and ML analyses but poorly supported in the species tree analysis (BI/MP/ML = 0.4/98/100). The Soconusco region in Chiapas where *Z. soconuscensis* occurs is believed to have been a primary Pleistocene floristic refuge (Toledo 1982), so this species may be the sole survivor of a once larger group of species eliminated from surrounding areas during Pleistocene glaciations. Alternatively, the species may have other close relatives in neighboring Guatemala, as on-site observations point to several as yet undescribed species of *Zamia* in the region. The potential discovery of related species and/or the inclusion of additional loci may aid in phylogenetic reconstructions to explain or reject the unusual placement recovered for *Z. soconuscensis* in our analyses.

Central-meridional clade. The Central-meridional clade (fig. 4, node I; BI/MP/ML = 0.98/99.6/98) includes more than 60% of all species in the genus, making it by far the most species-rich clade within the mainland zamias. It includes all species occurring from southern Nicaragua south to the southern limit of the genus's range in Brazil and Bolivia. It is separated by a large distribution gap from Mesoamerican *Zamia* populations, which only extend to northern Honduras and El Salvador. This group consists of two sister clades: one that is mainly species endemic to the Central American Isthmus (Isthmus clade) and another that is mainly South American species (South America clade).

Isthmus clade. The Isthmus clade (fig. 4, node J; BI/MP/ML = 1/99.9/100) consists of 15 species mostly restricted to the Central American Isthmus region, with only *Zamia obliqua* extending into Colombia in adjacent South America. Most species are arborescent, with only two (*Z. nana* and *Z. dressleri*) having subterranean stems. Notable groups within the Isthmus clade include the Acuminata subclade (fig. 4, node K; BI = 0.92) with four species restricted to the Pacific side of the Cordillera Central mountain range in Costa Rica and Panama, the Obliqua subclade (fig. 4, node L; BI/ML = 0.88/87), consisting of arborescent species with very sparsely armed petioles, and the Skinneri subclade (fig. 4, node M; BI/MP/ML = 0.83/100/100), composed of five arborescent species with large, broad, prominently veined leaflets and occurring primarily on the Atlantic side of the Cordillera Central from central Panama through southern Nicaragua. *Zamia dressleri*, a species with similar leaflet morphology but with a subterranean stem, has previously been considered part of the *Z. skinneri* Warsz. ex A.Dietr. species complex (Taylor et al. 2008), but this relationship was not supported by our analyses which recovered the species as sister to the Obliqua subclade.

South America clade. The South America clade (fig. 4, node N; BI/MP/ML = 1/100/100) consists of 28 species endemic to South America, with the exception of *Zamia manicata* Linden ex Regel, which extends into Panama, and sister species *Zamia cunaria* and *Zamia ipetiensis* (Cunaria clade; fig. 4, node R; BI = 0.89), which are Panamanian endemics. The phylogenetic relationship of the latter two species to other species occurring in South America remains unclear, as the phylogenetic analyses resulted in conflicting and poorly supported topologies. However, these species share extensive morphological similarities with *Zamia pyrophylla* from the Colombian Chocó, including subterranean stems holding only one to two leaves, tomentum present on strobili axes, and microsporangia on the adaxial side of the microsporophylls (Calonje et al. 2010).

The Manicata subclade (fig. 4, node O; BI/MP/ML = 1/99.3/100) is a group of four species occurring primarily in northern Colombia that have a remarkably variable leaflet morphology including the distinctly channeled petiolule with a gland-like collar of *Zamia manicata*, the membranaceous and prominently veined leaflets of *Zamia disodon* D.W.Stev. & Sabato, and the unusual midrib found in *Zamia restrepoi* (D.W.Stev.) A.Lindstr. The midrib found in *Z. restrepoi* leaflets is unique in the genus and so distinctive that the species was initially described within its own genus (*Chigua* D.W.Stev.) until it was eventually subsumed into *Zamia* (Lindstrom 2009). The strikingly diverse leaflet morphology found in this clade has historically obscured the close phylogenetic relationships of its constituent species, but they do share other characters such as acaulescent stems, toothed leaflets, relatively small seeds, and microsporophylls with a very short fertile section of lamina; these characters support the close relationship recovered in our analyses.

The Pacific subclade (fig. 4, node P; BI/MP/ML = 0.78/70/89) consists of five species occurring from the western foothills of the Andes to the Pacific coast. The species are variable in terms of leaflet vein prominence, stem habit, and leaflet margin dentation (figs. D1–D4) but are all extensively armed with prickles on the petioles, making it the most aggressively armed clade in the genus. Panamanian highland species *Zamia lindleyi* Warsz. Ex A.Dietr. was previously considered conspecific with *Zamia chigua* Seem. (Stevenson 1993) from the lowlands of the Colombian Chocó biogeographic region primarily due to having fernlike leaves with numerous narrow leaflets. However, several morphological and ecological differences in addition to the large geographic disjunction have since brought recognition of *Z. lindleyi* as a distinct and separate species from *Z. chigua* (Calonje et al. 2012*b*), a recognition supported by our analyses, which place the former within the Isthmus clade and the latter in the South America clade. Norstog (1980) believed that Pacific subclade species *Zamia roezlii* Linden (as *Z. chigua*; Norstog 1986) was the most primitive species in the genus because its stable rainforest habitat allowed it to retain what he considered primitive characters such as an arborescent habit, large spermatozoids, and a large asymmetrical karyotype. However, three of the four traits we examined for this species, including the arborescent habit, were not ancestral in our character state reconstructions (figs. D1–D4). Additionally, karyotype evolution in *Zamia* appears to be moving toward increased asymmetry with higher numbers of smaller chromosomes (Vovides and Olivares 1996; Olson and Gorelick 2011), meaning the large asymmetric karyotype of *Z. roezlii* is currently considered more derived than ancestral.

The Wallisii subclade (fig. 4, node Q; BI/MP/ML = 0.78/93/99) consists of *Zamia wallisii* Braun and *Zamia oligodonta* E. Calderón & D.W.Stev., two subterranean-stemmed montane species with prominently veined, extremely broad, coriaceaous leaflets and ovoid female cones with few, relatively large seeds, both occurring on the western flank of Colombia's Western Cordillera. *Zamia montana* Braun, an arborescent species that also has prominently veined leaflets and occurs in the same geo-

graphic region, was not sampled in this study but likely belongs to this subclade as well. In fact, *Z. montana* and *Z. oligodonta* were previously considered conspecific due to vegetative similarities (Lindstrom 2009), but recent field studies with the two species (Calonje et al. 2015) have clarified that the two species are significantly morphologically distinct (Calonje et al. 2015).

The Tolimensis subclade (fig. 4, node S; BI = 0.67) consists of sister species *Zamia tolimensis* Calonje, H.E.Esquivel & D.W.Stev. and *Zamia huilensis* Calonje, H.E.Esquivel & D.W.Stev., both endemic to Colombia and occurring in mountain ranges surrounding the Magdalena River Valley. The former occurs in the Central Cordillera, the latter in the Eastern Cordillera and the Colombian Massif. Both are arborescent species sharing considerable similarities in reproductive structures (Calonje et al. 2012*a*).

The Eastern subclade (fig. 4, node T; BI/MP/ML = 0.81/64/88) consists of species occurring in eastern Colombia and western Venezuela. All species occur to the east of the Andes mountain range with the exception of *Zamia encephalartoides* D.W.Stev., which occurs on the western side of the Cordillera Oriental mountain range. The taxon treated here as *Zamia lecontei* Ducke is from Amazonian Venezuela, following the species circumscription by Stevenson (2004). However, the type locality for this species is a great distance away in Brazil, and additional taxonomic work is required to determine whether Brazilian, Venezuelan, and Colombian populations of this species are truly conspecific.

The Amazonian subclade (fig. 4, node U; BI/MP/ML = 0.64/70/95), recovered with high support only in the ML analysis, consists of seven species endemic to the Amazon basin. *Zamia poeppigiana* Mart. & Eichler, a large arborescent Amazonian species, shares many morphological similarities with *Zamia lindenii* Regel ex André, which occurs on the Pacific side of the Andes. The two were previously considered conspecific (Stevenson 2001) until additional taxonomic work helped clarify morphological differences between them (Lindstrom 2009; Calonje et al. 2011). Their placement in the separate Pacific and Amazonian subclades in our analyses justify their recognition as separate species.

Ancestral Character States and Homoplasy of Macromorphological Vegetative Characters

Homoplasy was prevalent within all the macromorphological characters examined (i.e. arborescence, petiole armature, leaflet margin dentation, and leaflet vein prominence), and no single character or combination thereof appeared to be diagnostic for the major clades within *Zamia* (figs. D1–D4). This is in accordance with previous findings by Caputo et al. (2004), who found all characters from an extensive morphological and micromolecular data set to be homoplastic, as well as with inferences from population-based studies in the Caribbean clade (Salas-Leiva et al. 2017; Meerow et al. 2018). The rampant homoplasy pervasive in the genus has resulted in several species that share morphological resemblance but that are not closely related. This is perhaps best exemplified by species with prominently veined leaflets, a character unique to the genus and so distinctive that it was the primary reason for the segregation of the genus *Aulacophyllum* Regel from *Zamia* (Regel 1876). This character state, found in approximately one-quarter of all *Zamia* species, has evolved multiple times throughout the genus and is not diagnostic of any clade (fig. D4). Similarly, several large arborescent South American species with prominently toothed leaflet margins (*Zamia tolimensis*, *Z. lindenii*, and *Zamia poeppigiana*), which were previously considered to belong to the same species complex (Calonje et al. 2011), are actually members of three separate lineages within the South America clade. The pervasiveness of homoplasy within macromorphological vegetative characters typically considered informative complicates their diagnostic utility, and future systematic research will need to consider an array of characters, including morphological, anatomical, reproductive, and genetic characters.

Genome Sizes in Zamia

We recovered a strong phylogenetic signal for the evolution of genome size within the crown group of *Zamia* (Pagel's $\lambda = 0.97$), indicating a strong statistical dependence between DNA content and our species tree topology. Zonneveld and Lindström (2016) posited a southward migration of *Zamia* based on increasing genome size to the south. However, genome size appears to have evolved stochastically within the genus, with both increases and decreases in DNA content occurring in different clades. Zonneveld and Lindström (2016) noted patterns between genome size and geographic distribution, identifying three major biogeographic groups matching the Mesoamerican, Caribbean, and South and Central American areas of endemism (fig. 1) for the genus. However, the latter two groups are not diagnosable based on genome size alone, as they include overlapping values, a situation that Zonneveld and Lindström (2016) attributed to ancient hybridizations between the two groups. Our results instead suggest that these similarities are due to both groups having genome sizes that have remained stable since the diversification of the crown node of the genus (fig. D5). Similarly, the Mesoamerican group, while diagnosable by its low genome size, in our phylogenetic analyses represents a paraphyletic assembly that includes members of the separate Mesoamerica and Fischeri clades as well as *Zamia soconuscensis*.

Divergence Age Estimation

The divergence between *Zamia* and *Microcycas* was estimated to be 68.28 Ma (95% HPD 50.99–84.5), an estimate older than those presented by Condamine et al. (57 Ma), Salas et al. (36.5 Ma), and Nagalingum et al. (31.1 Ma). Our estimate suggests that the divergence between the two genera happened near the Cretaceous-Paleogene boundary, which was marked by the catastrophic Chicxulub asteroid impact that may have wiped out up to 60%–70% of plant species in tropical North America (Nichols and Johnson 2009). The impact likely had a devastating effect on contemporary cycad flora in the Americas, but the aftermath likely presented a speciation opportunity for surviving cycad lineages. The estimated stem age for *Microcycas* is older than the present Antillean islands, which were formed less than 40 Ma (i.e., late Eocene; Iturralde-Vinent 2006). This suggests the ancestral range of *Microcycas* may have originally included mainland populations that eventually became extinct. However, such interpretation should be taken cau-

tiously as the fossil record for *Zamia* is scarce and is, as yet, inexistent for *Microcycas*. As the latter is a monotypic genus, there are no diversification events to infer that could clarify its biogeographic history.

The mean crown age of *Zamia* was estimated at 9.54 Ma (95% HPD 9.0–10.6 Ma). This age is younger than reported by Condamine et al. (2015; 14.6 Ma, using new fossil data set and birth/death prior), slightly younger than reported by Nagalingum et al. (11.25 Ma, BI using nuclear markers), and slightly older than reported by Salas et al. (8.2 Ma). Our crown age estimate for *Zamia* marks the divergence of the Caribbean clade from the Mainland clade and is concordant with the time-since-divergence estimate (Sarich 1977) of 10.8 Ma between *Zamia pumila* L. (sensu Eckenwalder 1980*a*) and *Zamia splendens* reported by Walters and Decker-Walters (1991) based on allozyme differentiation. However, our use of a stem calibration for the genus represents a rather conservative approach that might push the age of the crown group toward the present. We thus suggest to interpret our estimates as minima that will be more properly resolved by employing more sophisticated ways of dealing with fossil information.

Biogeography of Zamia

Geographic delimitation of clades. Three separated major areas of endemism are readily identifiable in the geographic distribution of the genus *Zamia*: the Caribbean Islands and southeast United States, Mesoamerica, and Central and South America (fig. 1). The latter two groups are separated by a considerable distribution gap extending from northern Salvador/Honduras to southern Nicaragua. The *Zamia* species occurring in the Caribbean Islands and southeast United States are all monophyletic (Caribbean clade), as are all species from Central and South America (Central-meridional clade). However, in the Mesoamerica region we found two separate clades with overlapping geographic distributions (Fischeri and Mesoamerica clades) as well as the unusual situation with *Z. soconuscensis*, which in our analyses appears more closely related to the Central-meridional clade than to any Mesoamerican species. With the notable exception of *Z. soconuscensis*, we found a strong pattern of phylogenetic congruence with geographic distribution in *Zamia*, with most of the major clades recovered in our analyses exclusively occurring in particular geographic regions with little or no range overlap. Indeed, our results bolster similar findings by Caputo et al. (2004) by demonstrating that this pattern is widespread throughout the entire genus.

The strong congruence between geographic distribution and phylogenetic relationships recovered in our analysis is a pattern consistent with the limited dispersal and pollen-transfer abilities found in cycads (Tang 1993; Yang and Meerow 1996), which most likely limit the ability of these clades to expand beyond geographically contiguous and ecologically suitable conditions following isolation via vicariance or dispersal events. Although rare, long-range dispersal events have occurred, as evidenced by the distribution of Caribbean clade species on landmasses that have never had land connections between them, and these events have played a role in shaping the evolutionary history of the genus (Salas-Leiva et al. 2017). Eckenwalder (1980*b*) posited that overwater dispersal of Caribbean zamias could occur via beached rafts of drift material carried by strong currents or during hurricanes. Additionally, several authors have reported birds as short-range dispersal agents of *Zamia* (Eckenwalder 1980*b*; Gómez 1993; Tang 1993; Chemnick 2007). Long-range dispersal could also be possible via larger birds that are able to swallow whole seeds and disperse them via defecation, such as the great Curassow (*Crax rubra* L.), a known dispersal agent of *Ceratozamia whitelockiana* Chemnick & T.J.Greg. (Chemnick 2007). The distribution range of *Zamia*, by far the broadest in the New World cycads and including several landmasses never connected by land, suggests that its dispersal abilities have played an important role in its evolutionary history.

Historical biogeography of Zamia. Inferring the historical biogeography of *Zamia* with any certainty is burdened by an extremely poor fossil record consisting of a single fossil that can be unequivocally assigned to *Zamia* based on morphological and epidermal characters (Erdei et al. 2018). The fossil, estimated to be of late Eocene to earliest Oligocene age (ca. 33–35 Ma), was found in marine sediments in central Panama. Little is known about its terrestrial origin, but since parts of the Panama Arc were emergent since at least 30 Ma (O'Dea et al. 2016), it is possible that leaflets may have been carried by currents from nearby islands or more distant land. Interestingly, the cuticular micromorphology of the Panamanian fossil more closely resembles that of extant Caribbean clade species than that of Central-meridional clade species (Erdei et al. 2018). This may imply that the elongated adaxial cuticular cell shape and stomatal band width and ratio found in Caribbean species are ancestral character states. Two additional Paleogene (i.e., Oligocene 30 Ma) fossils from Collazo Shale (Puerto Rico) were originally described as separate species of *Zamia* (Hollick 1928) but are apparently conspecific (Erdei et al. 2018). Despite their *Zamia*-like macromorphology, their confirmation as *Zamia* is not possible due to poorly preserved cuticles (Erdei et al. 2018). If assignable to *Zamia*, the fossils would indicate the earlier presence of the genus in the Caribbean, albeit likely of an extinct lineage, as Puerto Rico was below sea level between the Late Oligocene and Early Pliocene (van Gestel et al. 1998). Hence, the current presence of *Zamia* on the island may be younger than ca. 5 Ma (Meerow et al. 2012), which is in agreement with our estimations suggesting that the diversification of extant Caribbean species occurred less than 2 Ma and within the last 340,000 yr for Puerto Rican and Dominican species (fig. 5).

The young age retrieved for the crown group of the Caribbean clade contrasts with its relatively old stem age, perhaps resulting from high turnover rates caused by glacio-eustatic sea level fluctuations, which can greatly influence island biotas (Weigelt et al. 2016). In fact, the effects of historic sea level fluctuations are readily observable in the genetic structure of extant species. Sea level fluctuations are thought to have reinforced isolation in *Zamia erosa* O.F.Cook & G.N.Collins limestone hill populations in northern Puerto Rico by eliminating intervening populations in the lowlands (Meerow et al. 2012). Similarly, populations of *Zamia* on five islands in the Bahamian archipelago cluster genetically into two groups (Salas-Leiva et al. 2017) that correspond to two separate historic landmasses (Little Bahamas Bank and Great Bahamas Bank), which encompassed these islands during the Last Glacial Maximum (33.0 and 26.5 Ka) when sea levels were as much as 120–135 m below current levels (Clark and Mix 2002).

Based on the limited fossil record for *Zamia*, Erdei et al. (2018) suggested an Eocene or earliest Oligocene origin of the genus in the Central American–Caribbean region with subsequent dispersal south and northward. Our molecular biogeographic and divergence time estimation analyses instead suggest an older Late Cretaceous to early Eocene origin for the stem group of *Zamia* and a Caribbean or Mesoamerican origin for both the stem and crown nodes of *Zamia* with subsequent dispersal of the genus south into the Central American Isthmus region and South America. Despite the discovery in the Central American Isthmus region of the only anatomically verified *Zamia* fossil (albeit of unknown terrestrial provenance), a Caribbean or Mesoamerican origin for the genus appears more convincing due to the presence of the sister genus *Microcycas* as well as the two earliest diverging *Zamia* lineages (Caribbean and Fisheri clades) at the northernmost range of the genus's geographic range. Our biogeographic analysis suggests a northern origin for the crown group of *Zamia* with vicariance caused by a southward distribution shift in the Late Miocene, a subepoch characterized by increasing drought, enhanced seasonality, and a restructuring of terrestrial biological communities (Herbert et al. 2016). Discoveries of additional fossils of *Zamia* or its sister genus *Microcycas* may help to better recreate the still poorly understood early biogeographic history of the genus.

There is currently considerable disagreement regarding dating of the emergence of the Panama land bridge, with several authors advocating the traditional view of ca. 2.8 Ma (O'Dea et al. 2016) and others suggesting the isthmus has been in place for more than 10 Ma (Montes et al. 2012; Jaramillo et al. 2017). Either way, the estimated divergence of the Central-meridional clade into the Isthmus and South America clades (3.8 Ma, 95% HPD 2.49–5.17) suggests that the two groups diverged when the Panama land bridge was either nearly completed (O'Dea et al. 2016) or had been in place for millions of years.

Diversification of the crown nodes for both clades began nearly simultaneously about a million years later, with the South America clade's mean crown age estimated at 2.62 Ma (95% HPD 1.71–3.56) and the Isthmus clade's at 2.35 Ma (95% HPD 1.43–3.32). This period coincides with the establishment of repeated Pleistocene glaciations beginning at 2.6 Ma, which converted much of Central America into recurrently dry environments (Bacon et al. 2016) leading to the fragmentation of wet forest habitat favored by the Central-meridional clade and likely driving diversification of both the Isthmus and South America clades.

The South America clade is considerably more species rich and has a broader geographic range than the Isthmus clade, perhaps in part because the dispersal potential of the latter has been limited by the geographic bottleneck of the isthmus's narrow landmass. Despite this bottleneck, the Isthmus clade has been remarkably successful. It has the third highest net diversification rate after the Caribbean and South America clades (table 8), and the Isthmus region hosts the greatest concentration of species per unit area in the genus, with the main taxonomic diversity hot spots occurring in central Panama and along the Costa Rican and Panamanian border (fig. 8).

The Isthmus and South America clades appear to have diversified and dispersed mostly within their geographic regions, despite the fact that this diversification occurred when the Panama land bridge was already present or near completed. The genetic isolation of these clades mirrors similar findings reported for birds (Smith and Klicka 2010) and mammals (Webb 1976) in which biotic interchange facilitated by uplift of the isthmus declined during the Pleistocene, perhaps driven by the unavailability of ecological space. Reduced migration by birds and mammals, both known dispersal agents of *Zamia* (Tang 1989), may have affected transisthmian dispersal of the genus, and the ecological niches available to *Zamia* may have also filled rapidly in both landmasses, therefore impeding biotic exchange. Finally, the coevolution of *Zamia* species with insect pollinators also may have played a role in keeping the clades separate. In fact, whereas erotylid beetle pollinators of the genus *Pharaxonotha* Reitter are found throughout most of the distribution range of *Zamia*, weevil pollinators of the subtribe *Allocorynina* Sharp are absent from South America clade species (O'Brien and Tang 2015).

Table 8

Net Diversification Rates of Major Clades Using Different Extinction Rates

Clade	*n*	Net diversification rates (ε) = 0	(ε) = .7	(ε) = .9
This study:				
Full tree	77	.03	.02	.02
Zamia stem	76	.05	.04	.03
Zamia crown	75	.39	.32	.22
Caribbean	9	1.26	.88	.45
Mainland	66	.60	.49	.34
Mesoamerica	18	.60	.46	.27
Fischeri	3	.16	.10	.05
Central-meridional	44	.82	.66	.43
Isthmus	16	.88	.65	.37
South America	28	1.04	.81	.50
Other studies:				
Gymnosperms (Crisp and Cook 2011)	18	.17	.12	.07
Zamia crown (Nagalingum et al. 2011)	31	.32	.27	.19
Zamia crown (Condamine et al. 2015)	43	.25	.21	.14

Note. Rates from other studies calculated based on inferred clade ages.

Diversification

Most diversification above the crown node of *Zamia* occurred in the Pliocene and Pleistocene epochs, with only the split between the Caribbean and Mainland clade and between the Fischeri clade and the rest of the Mainland clade occurring in the Miocene (figs. 5, 6). The vast majority of extant *Zamia* species appear to be of Pleistocene origin, suggesting that climactic oscillation during this epoch may have played a role in diversification.

The net diversification rates (sensu Magallon and Sanderson 2001) recovered for the crown group of *Zamia* are among the highest reported for gymnosperm genera by Crisp and Cook (2011), yet comparable to rates obtained using clade age estimates from Nagalingum et al. (2011) and Condamine et al. (2015; table 8). The diversification rates were highest in the

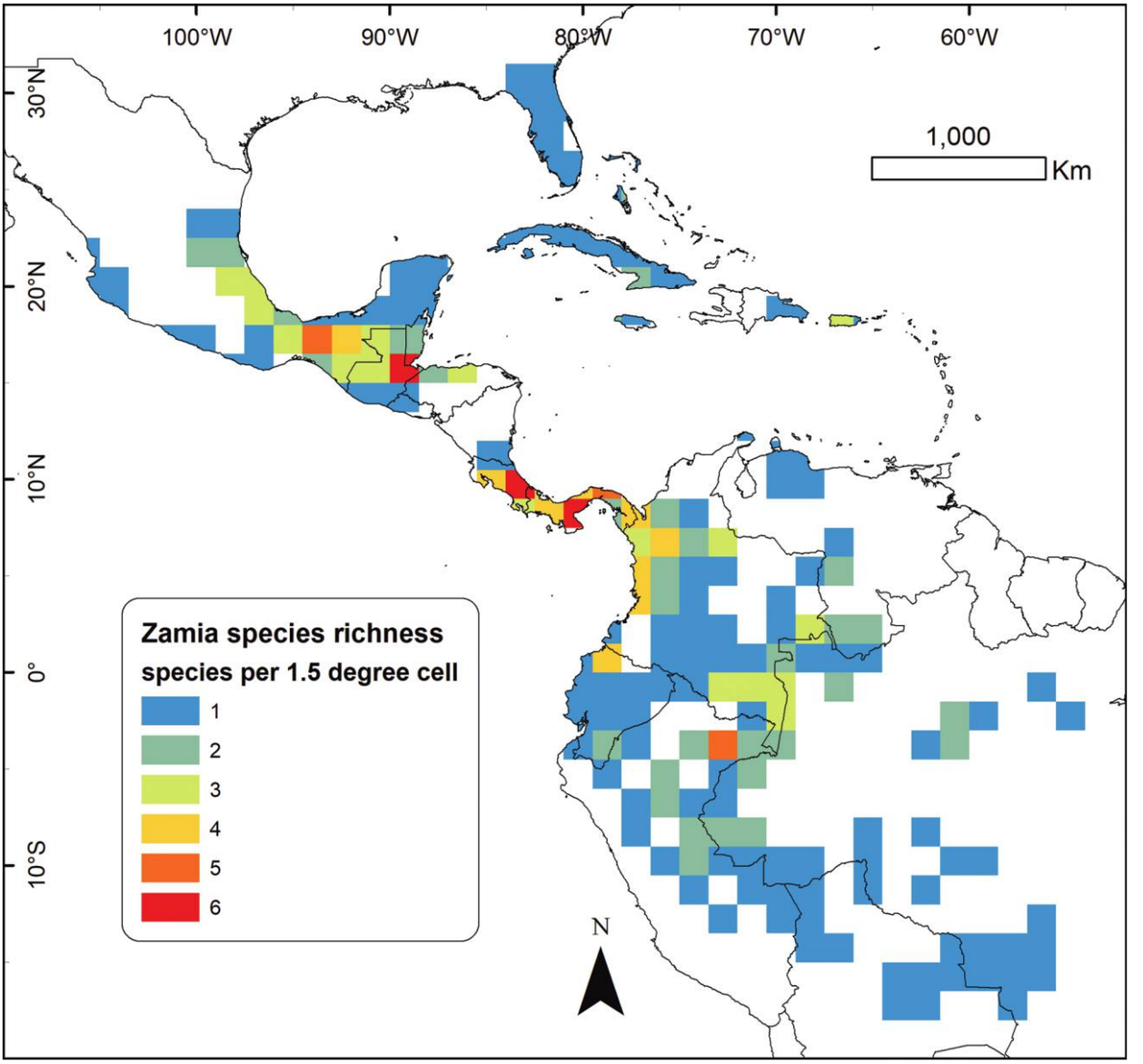

Fig. 8 Species richness of *Zamia*.

Caribbean clade, followed by the South America and Isthmus clades, the two major clades constituting the Central-meridional clade (table 8). The high diversification rate recovered in the Caribbean clade may be partly due to the very short generation times found in this clade, as its constituent species are able to reach reproductive age as early as 2 yr from seed (Salas-Leiva et al. 2017), therefore allowing for a faster rate of accumulation of neutral mutations compared with most mainland species.

It has been argued that the Magallon and Sanderson (2001) diversification rate estimate represents a more accurate estimator to infer rate shifts than BAMM (Meyer et al. 2018; Meyer and Wiens 2018). Indeed, our BAMM analysis suggests there is no significant variation in rate between clades. However, the difference in sample size between the clades identified here might indicate that the extreme estimates obtained for the two clades with the highest and lowest rates (Caribbean clade, $n = 9$, and Fischeri clade, $n = 3$) are very poor estimators of the subtending variation (Rabosky 2018). Thus, we advise that the results obtained here using the Magallon and Sanderson (2001) methods should be interpreted with caution. A similar issue might affect our estimation of the gamma statistic for different subclades.

Nagalingum et al. (2011) found patterns of early diversification followed by subsequent decreases in diversification rates for all cycad genera, a pattern typical of an adaptive radiation (Rabosky and Hurlbert 2015), which they attributed to newly available seasonal environments as the ecological opportunity that triggered a global radiation following the mid-Miocene transition. We found a signal for significant early rapid speciation only in the South America clade (fig. 6), perhaps an indication of adaptive radiation triggered by the ecological opportunity

Table 9

Species Diversity, γ Values, and Results of the Monte Carlo Constant Rates Test for Major Clades Studied

Clade	Total diversity, sampled diversity	% diversity sampled	Gamma statistic (γ)	Critical value of γ (at 5% level)	*P*
Full tree	82, 77	94	11.18	−1.79	1*
Zamia stem	81, 76	94	8.67	−1.78	1*
Zamia crown	80, 75	94	1.73	−1.36	.52
Caribbean	9, 9	100	.97	−1.62	.83
Mainland	71, 66	93	−.07	−1.77	.86
Mesoamerica	21, 18	86	.45	−1.79	.72
Fischeri	3, 3	100	.60	−1.54	.68
Central-meridional	46, 44	96	−1.24	−1.75	.12
Isthmus	16, 16	100	−.01	−1.63	.50
South America	30, 28	93	−1.84	−1.75	.04*

* *P* = where null model of constant diversification was rejected.

presented by newly colonized South America. All other clades had constant diversification rates following a "museum model" of evolution (Wallace 1878; Fischer 1960) with gradual species accumulation coupled with low extinction rates. This model is supported by the BAMM analysis, in which no significant diversification rate shifts were detected within *Zamia* or any of its constituent clades, and by the MCCR test, which indicated a constant diversification rate for the genus and most major clades (fig. 6; table 9). In addition, no significant mass extinction signals were detected in the genus using the Comet model (fig. D2). The stable diversification history apparent in *Zamia* differs from the findings of Yessoufou et al. (2014) in the genus *Encephalartos* Lehm., in which a mass extinction event has been postulated to explain a pattern of rate heterogeneity through time. This difference could indicate the ability of *Zamia* species to track their favorite habitat during periods of cooling-drying, or it could signify different patterns of cooling and aridification between Africa and the Neotropics (Couvreur 2015).

Conclusions

Our results suggest a crown age of ~10 Ma for the genus and an origin within the Mesoamerican or Caribbean region with eventual southward migration into the Central American Isthmus and South America. The diversification history of the genus appears relatively stable and characterized by gradual species accumulation and low extinction rates. Most extant *Zamia* species appear to have originated during the Pleistocene, suggesting an effect of climatic oscillations during this epoch on the diversification of the genus. We recovered a strong congruence between geographic distribution and phylogenetic relationships, a pattern consistent with the limited dispersal and pollen-transfer abilities found in cycads. Homoplasy was pervasive within macromorphological characters normally considered informative for the genus, suggesting that future classification work within the genus must rely mostly on genetic characters or explore a wider variety of potentially diagnostic characters, including additional morphological, anatomical, and reproductive characters. This study presents the most comprehensive interpretation of the evolutionary history of *Zamia* to date and should serve as a strong phylogenetic framework for subsequent research, including studies that may help increase our understanding of the mechanistic bases for the diversification of the genus. Future phylogenetic work, particularly with new high-throughput sequencing technologies, should help resolve some of the ambiguities that still remain in obtaining a fully resolved, well-supported phylogeny of the genus.

Acknowledgments

Funding for field and laboratory research was provided by the National Science Foundation (DEB 1050340), National Geographic Society (8965-11), Mohamed Bin Zayed Species Conservation Fund (project no. 0925331), Association for Zoological Horticulture, Institute of Museum and Library Services grants (MA-05-12-0336-12: Mission Based Collections Planning and MA-30-14-0123-14: Mission Based Collections Stewardship), SOS—Save Our Species (grant 2012A-035), Tinker Foundation Field Research Grant, Montgomery Botanical Center, US Department of Agriculture Agricultural Research Service, Fairchild Tropical Botanic Garden, Charles P and Dorothy Sacher, Dr. Lin Lougheed, and Christiane Tyson Research Fellowship granted to D. Salas-Leiva. We are grateful to the many botanic gardens, herbaria, and horticulturists that generously provided samples for this study (see app. A). Kyoko Nakamura provided laboratory training and support to M. Calonje; Fabien Condamine provided helpful guidance regarding age divergence estimation; and Miguel Angel Pérez Farrera provided relevant information about Mexican zamias. We are grateful to the two anonymous reviewers and to the editor Hervé Sauquet for helpful comments that allowed us to greatly improve previous versions of the manuscript. Finally, Claudia Patricia Gutierrez provided unconditional family support to M. Calonje during his dissertation work, from which this article originated.

Appendix A

Accessions Sampled for Molecular Analyses

The following information is provided for each sample: species name and authorship, sample ID, sample provenance or pedigree (country and state or province), representative herbarium specimen (collector, herbarium repository), DNA sample source (source and botanical garden accession numbers), Genbank accession numbers (from left to right, dashes indicate no sequence available: *40S*, *ATG2*, *CyAg*, *GroES*, *HTS*, *LiSH*, *PEX4*, *PMP22*, *psbK/I*, *WRKY4*. Herbarium acronyms follow Index

Herbariorum (http://sweetgum.nybg.org/science/ih/). Abbreviations used for DNA sample sources: FTBG: Fairchild Tropical Botanic Garden, HS: Herbarium specimen, JBC: Jardín Botánico Francisco Javier Clavijero, Xalapa, Veracruz, Mexico, LA: Harold Lyon Arboretum, Manoa, Hawaii, MBC: Montgomery Botanical Center, Coral Gables, FL, MS: Marie Selby Botanical Gardens, Sarasota, Florida, NN: Nong Nooch Tropical Botanical Garden, Pattaya, Thailand, USDA-ARS: US Department of Agriculture, Agricultural Resource Service (DNA repository), Miami, FL.

***Microcycas calocoma* (Miq.) A.DC.,** *Microcycas calocoma*, Cuba (Pinar del Rio), Calonje MBC12-006 (FTG), MBC 59875*B, MG148379, MG148494, MG148953, MG148609, MG148724, MG148838, MG149041, MG149183, MG149271, MG149413; ***Stangeria eriopus* (Kunze) Baill.,** *Stangeria eriopus* South Africa, Calonje MBC12-001(FTG), MBC 9868*C, -, MG148505, MG148964, MG148620, MG148735, -, MG149079, MG149194, MG149298, MG149424; ***Zamia acuminata* Oerst. ex Dyer,** *Zamia acuminata* CR1, Costa Rica (San José), Calonje et al. MAC04-001(1) (CR, FTG), MBC 20041004, MG148390, MG148516, MG148975, MG148631, MG148746, MG148849, MG149090, MG149205, MG149309, MG149435; ***Zamia acuminata* Oerst. ex Dyer,** *Zamia acuminata* CR2, Costa Rica (San José), Calonje et al. MAC04-001(1) (CR, FTG), MBC 20041004, MG148353, MG148527, MG148986, MG148642, MG148757, MG148860, MG149101, MG149216, MG149320, MG149446; ***Zamia amazonum* D.W.Stev.,** *Zamia amazonum* BR, Brazil (Amazonas), Madison & Kennedy 6563 (F, SEL, US), LA L-78.1374, MG148401, MG148538, MG148997, MG148653, MG148768, MG148871, MG149112, MG149227, MG149331, MG149457; ***Zamia amazonum* D.W.Stev.,** *Zamia amazonum* PE, Peru (Loreto), Lindstrom s.n. (FTG, L, V), NN, MG148412, MG148549, MG149008, MG148664, MG148779, MG148882, MG149123, MG149238, MG149342, MG149468; ***Zamia amplifolia* W.Bull ex Mast.,** *Zamia amplifolia*, Colombia (Valle del Cauca), Bogler 1223 (FTG), FTBG 91596, MG148423, MG148560, MG149019, MG148675, MG148790, MG148893, MG149134, MG149249, MG149353, MG149479; ***Zamia angustifolia* Jacq.,** *Zamia angustifolia* BS, Bahamas (Eleuthera), Calonje et al. BS10-200 (FTG, NY), USDA-ARS ZBE103, MG148434, MG148571, MG149030, MG148686, MG148801, MG148904, MG149145, MG149260, MG149364, MG149490; ***Zamia boliviana* (Brongn.) A.DC.,** *Zamia boliviana*, Bolivia, Little & Stevenson 1067 (FTG), MBC 981682*A, MG148445, MG148468, MG148927, MG148583, MG148698, MG148915, MG149042, MG149157, MG149375, MG149387; ***Zamia chigua* Seem.,** *Zamia chigua* 1, Colombia (Chocó), Wilder et al. s.n. (F), LA L-81.0783, MG148456, MG148479, MG148938, MG148594, MG148709, MG148813, MG149053, MG149168, MG149272, MG149398; ***Zamia chigua* Seem.,** *Zamia chigua* 2, Colombia (Valle del Cauca), Little & Stevenson 1068 (FTG), MBC 20010802*A, MG148354, MG148486, MG148945, MG148601, MG148716, MG148824, MG149060, MG149175, MG149283, MG149405; ***Zamia cremnophila* Vovides, Schutzman & Dehgan,** *Zamia cremnophila*, Mexico (Tabasco), Bogler 1225 (FTG), FTBG 87339C, MG148365, MG148487, MG148946, MG148602, MG148717, MG148830, MG149061, MG149176, MG149290, MG149406; ***Zamia cunaria* Dressler & D.W.Stev.,** *Zamia cunaria* 1, Panama (Panamá), Stevenson 1201 (FTG, NY, PMA, U), MBC 2000269*A, MG148371, MG148488, MG148947, MG148603, MG148718, MG148831, MG149062, MG149177, MG149291, MG149407; ***Zamia cunaria* Dressler & D.W.Stev.,** *Zamia cunaria* 2, Panama (Panamá), Stevenson 1201 (FTG, NY, PMA, U), MBC 2000311*A, MG148372, MG148489, MG148948, MG148604, MG148719, MG148832, MG149063, MG149178, MG149292, MG149408; ***Zamia decumbens* Calonje, Meerman, M.P.Griff. & Hoese,** *Zamia decumbens* 1, Belize (Toledo), Calonje et al. BZ08-201 (BRH, FTG, MO, NY, XAL), MBC 20080715, MG148373, MG148490, MG148949, MG148605, MG148720, MG148833, MG149064, MG149179, MG149293, MG149409; ***Zamia decumbens* Calonje, Meerman, M.P.Griff. & Hoese,** *Zamia decumbens* 2, Belize (Toledo), Calonje et al. BZ08-180 (FTG), MBC 20080676, MG148374, MG148491, MG148950, MG148606, MG148721, MG148834, MG149065, MG149180, MG149294, MG149410; ***Zamia disodon* D.W.Stev. & Sabato,** *Zamia disodon*, Colombia (Antioquia), Lindstrom s.n. (FTG, L, V), NN, MG148375, MG148492, MG148951, MG148607, MG148722, MG148835, MG149066, MG149181, MG149295, MG149411; ***Zamia dressleri* D.W.Stev.,** *Zamia dressleri* 1, Panama (Colón), Stevenson et al. 1145 (FTG), MBC 2000332*A, MG148376, MG148493, MG148952, MG148608, MG148723, MG148836, MG149067, MG149182, MG149296, MG149412; ***Zamia dressleri* D.W.Stev.,** *Zamia dressleri* 2, Panama (Kuna Yala), De Nevers, G. 6565 (STRI), SEL 1996-0009, MG148377, MG148495, MG148954, MG148610, MG148725, MG148837, MG149069, MG149184, MG149297, MG149414; ***Zamia elegantissima* Schutzman, Vovides & R.S.Adams,** *Zamia elegantissima* 1, Panama (Colón), Little & Stevenson 1149 (FTG), MBC 2000775*G, MG148378, MG148496, MG148955, MG148611, MG148726, MG148839, MG149070, MG149185, MG149299, MG149415; ***Zamia elegantissima* Schutzman, Vovides & R.S.Adams,** *Zamia elegantissima* 2, Panama (Kuna Yala), De Nevers & Henderson 6320 (MO), FTBG 93558*B, MG148380, MG148497, MG148956, MG148612, MG148727, MG148840, MG149071, MG149186, MG149300, MG149416; ***Zamia encephalartoides* D.W.Stev.,** *Zamia encephalartoides*, Colombia (Santander), Espinosa 2011-003 (FTG), MBC 94910*A, MG148381, MG148498, MG148957, MG148613, MG148728, MG148841, MG149072, MG149187, MG149301, MG149417; ***Zamia erosa* O.F.Cook & G.N.Collins,** *Zamia erosa* PR, Puerto Rico (Quebradillas), Meerow and Ayala-Silva 3100, USDA-ARS ZPR413, MG148382, MG148499, MG148958, MG148614, MG148729, MG148842, MG149073, MG149188, MG149302, MG149418; ***Zamia fairchildiana* L.D.Gómez,** *Zamia fairchildiana* CR, Costa Rica (Puntarenas), Liesner 2860 (CR, MO), MBC 20070835, MG148383, MG148500, MG148959, MG148615, MG148730, MG148843, MG149074, MG149189, MG149303, MG149419; ***Zamia fairchildiana* L.D.Gómez,** *Zamia fairchildiana* PA, Panama (Chiriquí), Michael Calonje MAC08-005 (PMA), MBC 20080102, MG148384, MG148501, MG148960, MG148616, MG148731, MG148844, MG149075, MG149190, MG149304, MG149420; ***Zamia fischeri* Miq.,** *Zamia fischeri* MX SLP, Mexico (San Luis Potosí), Nicolalde-Morejon 1620 (XAL), JBC 2008-089B, MG148385, MG148502, MG148961, MG148617, MG148732, MG148845, MG149076, MG149191, MG149305, MG149421; ***Zamia fischeri* Miq.,** *Zamia fischeri* MX SLP2, Mexico (San Luis Potosí), Calonje

FTG18-01 (FTG), FTBG 76845*A, MG148386, MG148503, MG148962, MG148618, MG148733, MG148846, MG149077, MG149192, MG149306, MG149422; ***Zamia fischeri* Miq.,** *Zamia fischeri* MX TAM, Mexico (Tamaulipas), Little & Stevenson 1070 (FTG), MBC 20010205, MG148387, MG148504, MG148963, MG148619, MG148734, MG148847, MG149078, MG149193, MG149307, MG149423; ***Zamia furfuracea* L.f.,** *Zamia furfuracea* 1, Mexico (Veracruz), Little & Stevenson 1098 (FTG), MBC 20010214*H, MG148388, MG148506, MG148965, MG148621, MG148736, MG148848, MG149080, MG149195, MG149308, MG149425; ***Zamia furfuracea* L.f.,** *Zamia furfuracea* 2, Mexico (Veracruz), Vovides 567 (XAL), MBC 99795*C, MG148389, MG148507, MG148966, MG148622, MG148737, MG148850, MG149081, MG149196, MG149310, MG149426; ***Zamia gentryi* Dodson,** *Zamia gentryi*, Ecuador (Esmeraldas), Luther et al. 1235 (SEL), MS 1995-0429 A, MG148391, MG148508, MG148967, MG148623, MG148738, MG148851, MG149082, MG149197, MG149311, MG149427; ***Zamia grijalvensis* Pérez-Farr., Vovides & Mart.-Camilo,** *Zamia grijalvensis*, Mexico (Chiapas), N. Martínez 246 (XAL), JBC 2009-018A, MG148392, MG148509, MG148968, MG148624, MG148739, MG148852, MG149083, MG149198, MG149312, MG149428; ***Zamia hamannii* A.S.Taylor, J.L.Haynes & Holzman,** *Zamia hamannii*, Panama (Bocas del Toro), Taylor et al. ASTB04-ZE1 (PMA), MBC 20040867*C, MG148393, MG148510, MG148969, MG148625, MG148740, MG148853, MG149084, MG149199, MG149313, MG149429; ***Zamia herrerae* S.Calderón & Standl.,** *Zamia herrerae* MX, Mexico (Chiapas), Calonje MBC18-01 (FTG), MBC 20010256*B, MG148394, MG148561, MG148970, MG148676, MG148791, MG148903, MG149135, MG149250, MG149365, MG149480; ***Zamia herrerae* S.Calderón & Standl.,** *Zamia herrerae* SV, El Salvador (Sonsonate), Bogler 1186 (FTG), FTBG 93423B, MG148395, MG148559, MG148971, MG148674, MG148789, MG148902, MG149133, MG149248, MG149363, MG149478; ***Zamia huilensis* Calonje, H.E.Esquivel & D.W.Stev.,** *Zamia huilensis*, Colombia (Huila), Little 9273 (US), HS, MG148396, MG148511, MG148972, MG148626, MG148741, MG148854, MG149085, MG149200, MG149314, MG149430; ***Zamia hymenophyllidia* D.W.Stev.,** *Zamia hymenophyllidia* PE, Peru (Loreto), Lindstrom s.n. (FTG, L, V), NN 16022A, MG148397, MG148512, MG148973, MG148627, MG148742, MG148855, MG149086, MG149201, MG149315, MG149431; ***Zamia imperialis* A.S.Taylor, J.L.Haynes & Holzman,** *Zamia imperialis* 1, Panama (Coclé), Taylor & Quirós ASTB01-LRica1 (PMA), MBC 2000401*A, MG148398, MG148513, MG148974, MG148628, MG148743, MG148856, MG149087, MG149202, MG149316, MG149432; ***Zamia imperialis* A.S.Taylor, J.L.Haynes & Holzman,** *Zamia imperialis* 2, Panama (Veraguas), Espinosa 2011-005 (FTG), MBC 2000266*A, MG148399, MG148514, MG148926, MG148629, MG148744, MG148857, MG149088, MG149203, MG149317, MG149433; ***Zamia incognita* A.Lindstr. & Idárraga,** *Zamia incognita*, Colombia (Antioquia), Lindstrom s.n. (FTG, L, V), NN, MG148400, MG148515, MG148976, MG148630, MG148745, MG148858, MG149089, MG149204, MG149318, MG149434; ***Zamia inermis* Vovides, J.D.Rees & Vázq.Torres,** *Zamia inermis*, Mexico (Veracruz), Espinosa 2011-006 (FTG), MBC 92143*D, MG148402, MG148517, MG148977, MG148632, MG148747, MG148859, MG149091, MG149206, MG149319, MG149436; ***Zamia integrifolia* L.f.,** *Zamia integrifolia* BS, Bahamas (Andros), Calonje & Meerow BS10-030.(FTG), USDA-ARS ZBA104, MG148403, MG148518, MG148978, MG148633, MG148748, MG148861, MG149092, MG149207, MG149321, MG149437; ***Zamia integrifolia* L.f.,** *Zamia integrifolia* CU, Cuba (Camaguey), Espinosa 2011-001 (FTG), MBC 9753*A, MG148404, MG148467, MG148979, MG148582, MG148697, MG148812, MG149068, MG149156, MG149322, MG149386; ***Zamia integrifolia* L.f.,** *Zamia integrifolia* US1, USA (Florida), Haynes JLH06-015 (FTG), MBC 20060452*A, MG148405, MG148519, MG148980, MG148634, MG148749, MG148862, MG149093, MG149208, MG149323, MG149438; ***Zamia integrifolia* L.f.,** *Zamia integrifolia* US2, USA (Florida), Haynes JLH05-284 (FTG), MBC 20050880*B, MG148406, MG148520, MG148981, MG148635, MG148750, MG148863, MG149094, MG149209, MG149324, MG149439; ***Zamia ipetiensis* D.W.Stev.,** *Zamia ipetiensis* 1, Panama (Kuna de Madungandí), Stevenson & Valdespinos 1159 (FTG, MO, NY, U), FTBG 89166, MG148407, MG148521, MG148982, MG148636, MG148751, MG148864, MG149095, MG149210, MG149325, MG149440; ***Zamia ipetiensis* D.W.Stev.,** *Zamia ipetiensis* 2, Panama (Kuna Yala), Calonje et al. MAC07-005 (PMA), MBC 20070592, MG148408, MG148522, MG148983, MG148637, MG148752, MG148865, MG149096, MG149211, MG149326, MG149441; ***Zamia ipetiensis* D.W.Stev.,** *Zamia ipetiensis* 3, Panama (Kuna de Wargandí), Calonje et al. MAC08-086 (PMA), MBC 20080111, MG148409, MG148523, MG148984, MG148638, MG148753, MG148866, MG149097, MG149212, MG149327, MG149442; ***Zamia lacandona* Schutzman & Vovides,** *Zamia lacandona*, Mexico (Chiapas), Bogler 1227 (FTG), FTBG 93932, MG148410, MG148526, MG148985, MG148641, MG148756, MG148869, MG149100, MG149215, MG149330, MG149445; ***Zamia lecointei* Ducke,** *Zamia lecointei* 1, Venezuela (Puerto Ayacucho), Bogler 1191 (FTG), Stevenson 1143 (U), FTBG 88497, MG148411, MG148528, MG148987, MG148643, MG148758, MG148870, MG149102, MG149217, MG149332, MG149447; ***Zamia lecointei* Ducke,** *Zamia lecointei* 2, Venezuela (Puerto Ayacucho), Bogler 1191 (FTG), Stevenson 1143 (U), FTBG 88500D, MG148413, MG148529, MG148988, MG148644, MG148759, MG148872, MG149103, MG149218, MG149333, MG149448; ***Zamia lindenii* Regel ex André,** *Zamia lindenii* 1, Ecuador (Esmeraldas), Espinosa 2011-007 (FTG), MBC 20001000*F, MG148414, MG148530, MG148989, MG148645, MG148760, MG148873, MG149104, MG149219, MG149334, MG149449; ***Zamia lindenii* Regel ex André,** *Zamia lindenii* 2, Ecuador (Los Rios), Gentry & Dodson 18045 (AUU, MO), FTBG 90351, MG148415, MG148531, MG148990, MG148646, MG148761, MG148874, MG149105, MG149220, MG149335, MG149450; ***Zamia lindleyi* Warsz. ex A.Dietr.,** *Zamia lindleyi*, Panama (Chiriquí), Calonje et al. PA08-123 (PMA), MBC 20010802*A, MG148416, MG148532, MG148991, MG148647, MG148762, MG148875, MG149106, MG149221, MG149336, MG149451; ***Zamia loddigesii* Miq.,** *Zamia loddigesii* MX CHP, Mexico (Chiapas), Espinosa 2011-002 (FTG), MBC 99801*A, MG148417, MG148533, MG148992, MG148648, MG148763, MG148876, MG149107, MG149222, MG149337, MG149452; ***Zamia loddigesii* Miq.,** *Zamia loddigesii* MX OAX, Mexico (Oaxaca), Walters TW-30-05 (XAL), MBC 93948*D, MG148418, MG148534, MG148993, MG148649,

MG148764, MG148877, MG149108, MG149223, MG149338, MG149453; ***Zamia loddigesii* Miq.,** *Zamia loddigesii* MX PUE, Mexico (Puebla), Calonje MBC18-02, MBC 99797*K, MG148419, MG148535, MG148994, MG148650, MG148765, MG148878, MG149109, MG149224, MG149339, MG149454; ***Zamia loddigesii* Miq.,** *Zamia loddigesii* MX SLP, Mexico (San Luis Potosí), -, MBC 2000797*A, MG148420, MG148536, MG148995, MG148651, MG148766, MG148879, MG149110, MG149225, MG149340, MG149455; ***Zamia loddigesii* Miq.,** *Zamia loddigesii* MX TAB, Mexico (Tabasco), A. Vovides 1347 (XAL), JBC 2000-036.01, MG148421, MG148537, MG148996, MG148652, MG148767, MG148880, MG149111, MG149226, MG149341, MG149456; ***Zamia loddigesii* Miq.,** *Zamia loddigesii* MX VER, Mexico (Veracruz), Stevenson et al. 538 (FTG), MBC 83311*B, MG148422, MG148539, MG148998, MG148654, MG148769, MG148881, MG149113, MG149228, MG149343, MG149458; ***Zamia lucayana* Britton,** *Zamia lucayana*, Bahamas (Long Island), Calonje et al. BS09-036 (FTG), USDA-ARS ZBLI228, MG148424, MG148540, MG148999, MG148655, MG148770, MG148883, MG149114, MG149229, MG149344, MG149459; ***Zamia macrochiera* D.W.Stev.,** *Zamia macrochiera*, Peru (Loreto), Plowman 7275 (F, GH), LA L-82.0862, MG148425, MG148541, MG149000, MG148656, MG148771, MG148884, MG149115, MG149230, MG149345, MG149460; ***Zamia manicata* Linden ex Regel,** *Zamia manicata* CO, Colombia (Antioquia), Stevenson et al. 604 (FTG, HUA), FTBG 84272*J, MG148426, MG148542, MG149001, MG148657, MG148772, MG148885, MG149116, MG149231, MG149346, MG149461; ***Zamia meermanii* Calonje,** *Zamia meermanii*, Belize (Belize), Calonje et al BZ08-152 (BRH, FTG, MO, NY, XAL), MBC 20080671, MG148427, MG148543, MG149002, MG148658, MG148773, MG148886, MG149117, MG149232, MG149347, MG149462; ***Zamia melanorrhachis* D.W.Stev.,** *Zamia melanorrhachis*, Colombia, Lindstrom s.n. (FTG, L, V), NN 13364B, MG148428, MG148544, MG149003, MG148659, MG148774, MG148887, MG149118, MG149233, MG149348, MG149463; ***Zamia muricata* Willd.,** *Zamia muricata* CO, Colombia (Meta), Lindstrom s.n. (L, V), NN, MG148429, MG148547, MG149004, MG148662, MG148777, MG148890, MG149121, MG149236, MG149351, MG149466; ***Zamia muricata* Willd.,** *Zamia muricata* VE1, Venezuela (Carabobo), H.E. Luther s.n. (SEL 075089), SEL 1995-0433R, MG148431, MG148545, MG149006, MG148660, MG148775, MG148888, MG149119, MG149234, MG149349, MG149464; ***Zamia muricata* Willd.,** *Zamia muricata* VE2, Venezuela (Carabobo), Bogler 1226 (FTG), FTBG 88495, MG148430, MG148546, MG149005, MG148661, MG148776, MG148889, MG149120, MG149235, MG149350, MG149465; ***Zamia nana* A.Lindstr., Calonje, D.W.Stev. & A.S.Taylor,** *Zamia nana* 1, Panama (Coclé), Bogler 1215 (FTG), FTBG 89159, MG148432, MG148548, MG149007, MG148663, MG148778, MG148891, MG149122, MG149237, MG149352, MG149467; ***Zamia nana* A.Lindstr., Calonje, D.W.Stev. & A.S.Taylor,** *Zamia nana* 2, Panama (Coclé), Stevenson & Valdespinos 1147 (FTG, PMA, MO), MBC 20020234*B, MG148433, MG148550, MG149009, MG148665, MG148780, MG148892, MG149124, MG149239, MG149354, MG149469; ***Zamia nesophila* A.S.Taylor, J.L.Haynes & Holzman,** *Zamia nesophila*, Panama (Bocas del Toro), N. Espinosa 2011-008 (FTG), MBC 20010123*A, MG148435, MG148551, MG149010, MG148666, MG148781, MG148894, MG149125, MG149240, MG149355, MG149470; ***Zamia neurophyllidia* D.W.Stev.,** *Zamia neurophyllidia* CR, Costa Rica, Burger 3877 (US), FTBG 91188, MG148436, MG148552, MG149011, MG148667, MG148782, MG148895, MG149126, MG149241, MG149356, MG149471; ***Zamia neurophyllidia* D.W.Stev.,** *Zamia neurophyllidia* PA, Panama (Bocas del Toro), Correa et al 3078 (PMA), MBC 20080327, MG148437, MG148553, MG149012, MG148668, MG148783, MG148896, MG149127, MG149242, MG149357, MG149472; ***Zamia obliqua* A.Braun,** *Zamia obliqua* CO, Colombia (Chocó), Kiem & Norstog 36 (FTG), HS, MG148438, MG148554, MG149013, MG148669, MG148784, MG148897, MG149128, MG149243, MG149358, MG149473; ***Zamia obliqua* A.Braun,** *Zamia obliqua* PA1, Panama (Panamá), Calonje & Taylor PA09-020 (FTG), cult. Greg Holzman, MG148439, MG148555, MG149014, MG148670, MG148785, MG148898, MG149129, MG149244, MG149359, MG149474; ***Zamia obliqua* A.Braun,** *Zamia obliqua* PA2, Panama (Panamá), Bogler 1240 (FTG), FTBG 89162, MG148440, MG148556, MG149015, MG148671, MG148786, MG148899, MG149130, MG149245, MG149360, MG149475; ***Zamia oligodonta* E.Calderón & D.W.Stev.,** *Zamia oligodonta*, Colombia (Risaralda), Calderón-Sáenz 183 (NY), Cult. T. Maerowitz, MG148441, MG148557, MG149016, MG148672, MG148787, MG148900, MG149131, MG149246, MG149361, MG149476; ***Zamia onan-reyesii* C.Nelson & Sandoval,** *Zamia onan-reyesii*, Honduras (Cortés), Haynes et al. JLH03-045 (TEFH), MBC 20030887*V, MG148442, MG148558, MG149017, MG148673, MG148788, MG148901, MG149132, MG149247, MG149362, MG149477; ***Zamia paucijuga* Wieland,** *Zamia paucijuga* MX GRO, Mexico (Guerrero), Vovides et al. 1426 (XAL), MBC 20040444, MG148443, MG148562, MG149018, MG148677, MG148792, MG148905, MG149136, MG149251, MG149366, MG149481; ***Zamia paucijuga* Wieland,** *Zamia paucijuga* MX JAL, Mexico (Jalisco), Avendaño et al. 5255 (XAL), MBC 2000802*A, MG148444, MG148563, MG149020, MG148678, MG148793, MG148906, MG149137, MG149252, MG149367, MG149482; ***Zamia paucijuga* Wieland,** *Zamia paucijuga* MX OAX, Mexico (Oaxaca), Bogler 1198 (FTG), FTBG 931059, MG148446, MG148564, MG149021, MG148679, MG148794, MG148907, MG149138, MG149253, MG149368, MG149483; ***Zamia poeppigiana* Mart. & Eichler,** *Zamia poeppigiana*, Peru (Huanuco), Calonje D3 (FTG), cult. L. Whitelock, MG148447, MG148567, MG149022, MG148682, MG148797, MG148910, MG149141, MG149256, MG149371, MG149486; ***Zamia portoricensis* Urb.,** *Zamia portoricensis*, Puerto Rico, Meerow & Ayala-Silva 3105 (FTG), USDA-ARS ZPR713, MG148448, MG148568, MG149023, MG148683, MG148798, MG148911, MG149142, MG149257, MG149372, MG149487; ***Zamia prasina* W.Bull,** *Zamia prasina* BZ, Belize (Cayo), Calonje et al. BZ08-009 (FTG), MBC 20080682, MG148449, MG148569, MG149024, MG148684, MG148799, MG148912, MG149143, MG149258, MG149373, MG149488; ***Zamia prasina* W.Bull,** *Zamia prasina* GU, Guatemala (Petén), Calonje FTBG18-01 (FTG), FTBG 941079, MG148450, MG148570, MG149025, MG148685, MG148800, MG148913, MG149144, MG149259, MG149374, MG149489; ***Zamia prasina* W.Bull,** *Zamia prasina* MX CHI, Mexico (Chiapas), Hubbuch & Walters 172C (FTG), FTBG 93931A, MG148451, MG148572, MG149026, MG148687, MG148802, MG148914, MG149146, MG149261,

MG149376, MG149491; ***Zamia prasina* W.Bull,** *Zamia prasina* MX ROO, Mexico (Quintana Roo), Vovides et al. 1312 (XAL), MBC 2000799*A, MG148452, MG148573, MG149027, MG148688, MG148803, MG148916, MG149147, MG149262, MG149377, MG149492; ***Zamia prasina* W.Bull,** *Zamia prasina* MX YUC, Mexico (Yucatán), Vovides 856 (XAL), MBC 73385*B, MG148453, MG148574, MG149028, MG148689, MG148804, MG148917, MG149148, MG149263, MG149378, MG149493; ***Zamia pseudomonticola* L.D.Gómez ex D.W.Stev. & Sabato,** *Zamia pseudomonticola* CR, Costa Rica (Puntarenas), Calonje MAC04-012 (FTG), MBC 20041063, MG148454, MG148575, MG149029, MG148690, MG148805, MG148918, MG149149, MG149264, MG149379, MG149494; ***Zamia pseudomonticola* L.D.Gómez ex D.W.Stev. & Sabato,** *Zamia pseudomonticola* PA, Panama (Chiriquí), Espinosa 2011-004 (FTG), MBC 20020247*B, MG148455, MG148576, MG149031, MG148691, MG148806, MG148919, MG149150, MG149265, MG149380, MG149495; ***Zamia pseudoparasitica* J.Yates,** *Zamia pseudoparasitica* 1, Panama (Coclé), Stevenson DWS1206A (FTG, PMA, NY), MBC 2000319*A, MG148457, MG148577, MG149032, MG148692, MG148807, MG148920, MG149151, MG149266, MG149381, MG149496; ***Zamia pseudoparasitica* J.Yates,** *Zamia pseudoparasitica* 2, Panama (Veraguas), Kiem & Norstog 61 (FTG), FTBG 76663, MG148458, MG148578, MG149033, MG148693, MG148808, MG148921, MG149152, MG149267, MG149382, MG149497; ***Zamia pumila* L.,** *Zamia pumila* DR, Domican Republic, Calonje et al. DR09-001 (FTG), USDA-ARS ZDR111, MG148459, MG148579, MG149034, MG148694, MG148809, MG148922, MG149153, MG149268, MG149383, MG149498; ***Zamia purpurea* Vovides, J.D.Rees & Vázq.Torres,** *Zamia purpurea*, Mexico (Oaxaca), Bogler 1197 (FTG), FTBG 93928, MG148460, MG148580, MG149035, MG148695, MG148810, MG148923, MG149154, MG149269, MG149384, MG149499; ***Zamia pygmaea* Sims,** *Zamia pygmaea*, Cuba (Isla de la Juventud), Calonje D2 (FTG), Cult. Loran Whitelock, MG148461, MG148581, MG149036, MG148696, MG148811, MG148924, MG149155, MG149270, MG149385, MG149500; ***Zamia pyrophylla* Calonje, D.W.Stev. & A.Lindstr.,** *Zamia pyrophylla*, Colombia (Chocó), Kress & Echeverry 89-2571 (US), MBC 20100027*A, MG148462, MG148469, MG149037, MG148584, MG148699, MG148925, MG149043, MG149158, MG149273, MG149388; ***Zamia restrepoi* (D.W.Stev.) A.Lindstr.,** *Zamia restrepoi*, Colombia (Cordoba), Calonje MBC18-03 (FTG), MBC 20100026*A, MG148463, MG148470, MG149038, MG148585, MG148700, MG148814, MG149044, MG149159, MG149274, MG149389; ***Zamia roezlii* Linden,** *Zamia roezlii* CO, Colombia (Valle del Cauca), Bogler 1224 (FTG), FTBG 94909, MG148464, MG148471, MG149039, MG148586, MG148701, MG148815, MG149045, MG149160, MG149275, MG149390; ***Zamia roezlii* Linden,** *Zamia roezlii* EC, Ecuador (Esmeraldas), Janovec et al. 1285 (NY), MBC 20001005*N, MG148465, MG148472, MG149040, MG148587, MG148702, MG148816, MG149046, MG149161, MG149276, MG149391; ***Zamia sandovalii* C.Nelson,** *Zamia sandovalii*, Honduras (Atlántida), Calonje MBC18-04 (FTG), MBC 95744*B, MG148466, MG148473, MG148928, MG148588, MG148703, MG148817, MG149047, MG149162, MG149277, MG149392; ***Zamia skinneri* Warsz. ex A.Dietr.,** *Zamia skinneri*, Panama (Bocas del Toro), Calonje MBC18-05 (FTG), MBC 20010794*A, MG148355, MG148474, MG148929, MG148589, MG148704, MG148818, MG149048, MG149163, MG149278, MG149393; ***Zamia soconuscensis* Schutzman, Vovides & Dehgan,** *Zamia soconuscensis*, Mexico (Chiapas), Bogler 1185 (FTG), FTBG 88313, MG148356, MG148475, MG148930, MG148590, MG148705, MG148819, MG149049, MG149164, MG149279, MG149394; ***Zamia sp.,*** *Zamia sp.* PE SAM, Peru (San Martin), S. W. Ingram 1953 (SEL), MS 1981-2029*B, MG148360, MG148477, MG148934, MG148592, MG148707, MG148821, MG149051, MG149166, MG149281, MG149396; ***Zamia spartea* A.DC.,** *Zamia spartea*, Mexico (Oaxaca), Walters et al. 9-3 (XAL), MBC 93927*J, MG148357, MG148476, MG148931, MG148591, MG148706, MG148820, MG149050, MG149165, MG149280, MG149395; ***Zamia splendens* Schutzman,** *Zamia splendens* 1, Mexico (Chiapas), Walters 2001-37-B (XAL), MBC 20010267*A, MG148358, MG148524, MG148932, MG148639, MG148754, MG148867, MG149098, MG149213, MG149328, MG149443; ***Zamia splendens* Schutzman,** *Zamia splendens* 2, Mexico (Tabasco), Hubbuch & Walters 171 (FTG), FTBG 93930A, MG148359, MG148525, MG148933, MG148640, MG148755, MG148868, MG149099, MG149214, MG149329, MG149444; ***Zamia standleyi* Schutzman,** *Zamia standleyi*, Honduras (Cortés), Calonje FTBG18-02 (FTG), FTBG 65990C, MG148361, MG148478, MG148935, MG148593, MG148708, MG148822, MG149052, MG149167, MG149282, MG149397; ***Zamia stevensonii* A.S.Taylor & Holzman,** *Zamia stevensonii*, Panama (Panamá), Little & Stevenson 1168 (FTG), MBC 99885*A, MG148362, MG148480, MG148936, MG148595, MG148710, MG148823, MG149054, MG149169, MG149284, MG149399; ***Zamia tolimensis* Calonje, H.E.Esquivel & D.W.Stev.,** *Zamia tolimensis*, Colombia (Tolima), Little 8758 (US), HS, MG148363, MG148481, MG148937, MG148596, MG148711, MG148825, MG149055, MG149170, MG149285, MG149400; ***Zamia tuerckheimii* Donn.Sm.,** *Zamia tuerckheimii*, Guatemala (Alta Verapaz), Little & Stevenson 1163 (FTG), FTBG 771002B, MG148364, MG148482, MG148939, MG148597, MG148712, MG148826, MG149056, MG149171, MG149286, MG149401; ***Zamia urep* B.Walln.,** *Zamia urep*, Peru (Huánuco), Lindstrom s.n. (FTG, L, V), NN 15223A, MG148366, MG148483, MG148940, MG148598, MG148713, MG148827, MG149057, MG149172, MG149287, MG149402; ***Zamia variegata* Warsz.,** *Zamia variegata* BZ, Belize (Toledo), Calonje et al. BZ08-175 (FTG), MBC 20080675, MG148367, MG148565, MG148941, MG148680, MG148795, MG148908, MG149139, MG149254, MG149369, MG149484; ***Zamia variegata* Warsz.,** *Zamia variegata* GU, Guatemala (Izabal), Standley 23873 (US), FTBG 73196, MG148368, MG148566, MG148942, MG148681, MG148796, MG148909, MG149140, MG149255, MG149370, MG149485; ***Zamia vazquezii* D.W.Stev., Sabato & De Luca,** *Zamia vazquezii* MX VER, Mexico (Veracruz), Gonzalo Castillo CC4480 (XAL), JBC 1986-003, MG148369, MG148484, MG148943, MG148599, MG148714, MG148828, MG149058, MG149173, MG149288, MG149403; ***Zamia wallisii* Braun,** *Zamia wallisii*, Colombia (Antioquia), Little & Stevenson 1165 (FTG), MBC 20010301*A, MG148370, MG148485, MG148944, MG148600, MG148715, MG148829, MG149059, MG149174, MG149289, MG149404.

Literature Cited

Acuña-Castillo R, W Marín-Méndez 2013 Comparative anatomy of leaflets of *Zamia acuminata* and *Z. pseudomonticola* (Zamiaceae) in Costa Rica. Rev Biol Trop 61:539–546.

Bacon CD, P Molnar, A Antonelli, AJ Crawford, C Montes, MC Vallejo-Pareja 2016 Quaternary glaciation and the Great American Biotic Interchange. Geology 44:375–378.

Bogler DJ, J Francisco-Ortega 2004 Molecular systematic studies in cycads: evidence from *trn*L intron and ITS2 rDNA sequences. Bot Rev 70:260–273.

Bouckaert R, J Heled, D Kühnert, T Vaughan, C-H Wu, D Xie, MA Suchard, A Rambaut, AJ Drummond 2014 BEAST 2: a software platform for Bayesian evolutionary analysis. PLoS Comput Biol 10:e1003537.

Bouckaert RR, AJ Drummond 2017 bModelTest: Bayesian phylogenetic site model averaging and model comparison. BMC Evol Biol 17:42.

Calonje M, HE Esquivel, G Morales, YA Mora-Lizcano, D Stevenson 2012*a* A new arborescent species of *Zamia* (Cycadales, Zamiaceae) from the department of Huila, Eastern Cordillera of Colombia. Caldasia 34:283–290.

Calonje M, HE Esquivel, DW Stevenson, C Calonje, D Pava 2011 A new arborescent species of *Zamia* from the Central Cordillera of Tolima, Colombia (Cycadales, Zamiaceae), with comments on the *Z. poeppigiana* species complex. Brittonia 63:442–451.

Calonje M, G Morales, C López-Gallego, F Roldán 2015 A taxonomic revision of *Zamia montana* and *Zamia oligodonta*, with notes on their conservation status Phytotaxa 192:279–289.

Calonje M, DW Stevenson, C Calonje, YA Ramos, A Lindstrom 2010 A new species of *Zamia* from Choco, Colombia (Cycadales, Zamiaceae). Brittonia 62:80–85.

Calonje M, DW Stevenson, R Osborne 2019 The world list of cycads, online edition. http://cycadlistorg.

Calonje M, AS Taylor-Blake, D Stevenson, G Holzman, YA Ramos 2012*b* *Zamia lindleyi*: a misunderstood species from the highlands of western Panama. Mem N Y Bot Gard 106:419–437.

Caputo P, S Cozzolino, L Gaudio, A Moretti, DW Stevenson 1996 Karyology and phylogeny of some Mesoamerican species of *Zamia* (Zamiaceae). Am J Bot 83:1513–1520.

——— 2004 Molecular phylogeny of *Zamia* (Zamiaceae). Pages 149–157 *in* TW Walters, R Osborne, eds. Cycad classification: concepts and recommendations. CABI, Wallingford, UK.

Chaw SM, TW Walters, CC Chang, SH Hu, SH Chen 2005 A phylogeny of cycads (Cycadales) inferred from chloroplast *matK* gene, *trnK* intron, and nuclear rDNA ITS region. Mol Phylogenet Evol 37:214–234.

Chemnick J 2007 Seed dispersal agents of two Mexican cycads. Mem N Y Bot Gard 97:104–119.

Chernomor O, A von Haeseler, BQ Minh 2016 Terrace aware data structure for phylogenomic inference from supermatrices. Syst Biol 65:997–1008.

Clark PU, AC Mix 2002 Ice sheets and sea level of the Last Glacial Maximum. Quat Sci Rev 21:1–7.

Clugston JAR, MP Griffith, GJ Kenicer, CE Husby, MA Calonje, DW Stevenson, DP Little 2016 *Zamia* (Zamiaceae) phenology in a phylogenetic context: does in situ reproductive timing correlate with ancestry? Edinb J Bot 73:345–370.

Condamine FL, NS Nagalingum, CR Marshall, H Morlon 2015 Origin and diversification of living cycads: a cautionary tale on the impact of the branching process prior in Bayesian molecular dating. BMC Evol Biol 15:65.

Couvreur TLP 2015 Odd man out: why are there fewer plant species in African rain forests? Plant Syst Evol 301:1299–1313.

Crisp MD, LG Cook 2011 Cenozoic extinctions account for the low diversity of extant gymnosperms compared with angiosperms. New Phytol 192:997–1009.

Duncan WH 1979 *Zamia* (Cycadaceae) new for Georgia. Sida 8:115–116.

Eckenwalder JE 1980*a* Taxonomy of the West Indian cycads. J Arnold Arbor Harv Univ 61:701–722.

——— 1980*b* Dispersal of the West Indian cycad, *Zamia pumila* L. Biotropica 12:79–80.

Erdei B, M Calonje, A Hendy, N Espinoza 2018 A review of the Cenozoic fossil record of the genus *Zamia* L. (Zamiaceae, Cycadales) with recognition of a new species from the late Eocene of Panama: evolution and biogeographic inferences. Bull Geosci 93:185–204.

Escalante T, JJ Morrone, G Rodríguez-Tapia 2013 Biogeographic regions of North American mammals based on endemism. Biol J Linn Soc 110:485–499.

Farris JS, VA Albert, M Källersjö, D Lipscomb, AG Kluge 1996 Parsimony jackknifing outperforms neighbor-joining. Cladistics 12:99–124.

Fischer AG 1960 Latitudinal variations in organic diversity. Evolution 14:64–81.

Foote M 2000 Origination and extinction components of taxonomic diversity: general problems. Paleobiology 26:74–102.

Gómez LD 1993 Birds as short range seed dispersers of *Zamia fairchildiana* in SW Costa Rica. Rev Biol Trop 41:905–906.

González-Géigel L 2003 Zamiaceae. Pages 3–22 *in* Flora de la República de Cuba. Vol 4. AR Gantner KG, Liechtenstein.

Griffith M, M Calonje, D Stevenson, C Husby, D P. Little 2012 Time, place, and relationships: cycad phenology in a phylogenetic and biogeographic context. Mem N Y Bot Gard 106:59–81.

Harmon LJ, JT Weir, CD Brock, RE Glor, W Challenger 2008 GEIGER: investigating evolutionary radiations. Bioinformatics 24: 129–131.

Heled J, AJ Drummond 2010 Bayesian inference of species trees from multilocus data. Mol Biol Evol 27:570–580.

Herbert TD, KT Lawrence, A Tzanova, LC Peterson, R Caballero-Gill, CS Kelly 2016 Late Miocene global cooling and the rise of modern ecosystems. Nat Geosci 9:843–847.

Hill KD 1995 Infrageneric relationships, phylogeny and biogeography of the genus *Cycas* (Cycadaceae). Pages 139–162 *in* P Vorster, ed. Cycad 93, The 3rd International Conference on Cycad Biology, Proceedings. Cycad Society of South Africa, Stellenbosch.

Hill KD 1996 A taxonomic revision of the genus *Cycas* (Cycadaceae) in Australia. Telopea 7:1–63.

Hodell DA, JH Curtis, FJ Sierro, ME Raymo 2001 Correlation of Late Miocene to Early Pliocene sequences between the Mediterranean and North Atlantic. Paleoceanography 16:164–178.

Höhna S, MR May, BR Moore 2016 TESS: an R package for efficiently simulating phylogenetic trees and performing Bayesian inference of lineage diversification rates. Bioinformatics 32:789–791.

Hollick A 1928 Paleobotany of Porto Rico. Scientific survey of Porto Rico and the Virgin Islands. Vol 7. New York Academy of Sciences, New York.

Iturralde-Vinent MA 2006 Meso-Cenozoic Caribbean paleogeography: implications for the historical biogeography of the region. Int Geol Rev 48:791–827.

Jaramillo C, C Montes, A Cardona, D Silvestro, A Antonelli, CD Bacon 2017 Comment (1) on "Formation of the Isthmus of Panama" by O'Dea et al. Sci Adv 3:e1602321.

Johnson L 1959 The families of cycads and the Zamiaceae of Australia. Proc Linn Soc N S W 84:64–117.

Kalyaanamoorthy S, BQ Minh, TKF Wong, A von Haeseler, LS Jermiin 2017 ModelFinder: fast model selection for accurate phylogenetic estimates. Nat Methods 14:587.

Katoh K, DM Standley 2013 MAFFT Multiple sequence alignment software version 7: improvements in performance and usability. Mol Biol Evol 30:772–780.

Lahaye R, M van der Bank, D Bogarin, J Warner, F Pupulin, G Gigot, O Maurin, S Duthoit, TG Barraclough, V Savolainen 2008 DNA barcoding the floras of biodiversity hotspots. Proc Natl Acad Sci USA 105:2923–2928.

Lindstrom AJ 2009 Typification of some species names in *Zamia* L. (Zamiaceae), with an assessment of the status of *Chigua* D. Stev. Taxon 58:265–270.

Maddison W, DR Maddison 2017 Mesquite: a modular system for evolutionary analysis. Version 3.2. http://www.mesquiteproject.org.

Magallon S, MJ Sanderson 2001 Absolute diversification rates in angiosperm clades. Evolution 55:1762–1780.

Matzke NJ. 2013. BioGeoBEARS: biogeography with Bayesian (and likelihood) evolutionary analysis in R scripts R package, version 02. Vol 1. University of California, Berkeley.

May MR, S Höhna, BR Moore 2016 A Bayesian approach for detecting the impact of mass-extinction events on molecular phylogenies when rates of lineage diversification may vary. Methods Ecol Evol 7:947–959.

Meerow AW, J Francisco-Ortega, M Calonje, MP Griffith, T Ayala-Silva, DW Stevenson, K Nakamura 2012 *Zamia* (Cycadales: Zamiaceae) on Puerto Rico: asymmetric genetic differentiation and the hypothesis of multiple introductions. Am J Bot 99:1828–1839.

Meerow AW, DE Salas-Leiva, M Calonje, J Francisco-Ortega, MP Griffith, K Nakamura, F Jiménez-Rodríguez, J Lawrus, A Oberli 2018 Contrasting demographic history and population structure of *Zamia* (Cycadales: Zamiaceae) on six islands of the Greater Antilles suggests a model for population diversification in the Caribbean. Int J Plant Sci 179:730–757.

Meerow AWS, DW Moynihan, J Francisco-Ortega 2007 Unlocking the coontie conundrum: the potential of microsatellite DNA studies in the Caribbean *Zamia pumila* complex (Zamiaceae). Mem N Y Bot Gard 98:484–518.

Meyer ALS, C Román-Palacios, JJ Wiens 2018 BAMM gives misleading rate estimates in simulated and empirical datasets. Evolution 72:2257–2266.

Meyer ALS, JJ Wiens 2018 Estimating diversification rates for higher taxa: BAMM can give problematic estimates of rates and rate shifts. Evolution 72:39–53.

Miller MA, W Pfeiffer, T Schwartz 2011 The CIPRES science gateway: a community resource for phylogenetic analyses Proceedings of the 2011 TeraGrid Conference: Extreme Digital Discovery. ACM, Salt Lake City, UT.

Montes C, A Cardona, R McFadden, SE Moron, CA Silva, S Restrepo-Moreno, DA Ramirez, et al 2012 Evidence for middle Eocene and younger land emergence in central Panama: implications for isthmus closure. Geol Soc Am Bull 124:780–799.

Morrison DA 2009 A framework for phylogenetic sequence alignment. Plant Syst Evol 282:127–149.

Morrone JJ 2014 Biogeographical regionalisation of the Neotropical region. Zootaxa 3782:1–110.

Nagalingum NS, CR Marshall, TB Quental, HS Rai, DP Little, S Mathews 2011 Recent synchronous radiation of a living fossil. Science 334:796–799.

Nichols DJ, KR Johnson 2009 Plants and the K-T boundary. Cambridge University Press, Cambridge.

Nicolalde-Morejón F, F Vergara-Silva, J Gonzalez-Astorga, DW Stevenson 2010 Character-based, population-level DNA barcoding in Mexican species of *Zamia* L. (Zamiaceae: Cycadales). Mitochondrial DNA 21:51–59.

Nicolalde-Morejón F, F Vergara-Silva, J Gonzalez-Astorga, DW Stevenson, AP Vovides, V Sosa 2011 A character-based approach in the Mexican cycads supports diverse multigene combinations for DNA barcoding. Cladistics 27:150–164.

Nicolalde-Morejón F, AP Vovides, DW Stevenson, V Sosa 2008 The identity of *Zamia katzeriana* and *Z. verschaffeltii* (Zamiaceae). Brittonia 60:38–48.

Norstog K 1980 Chromosome numbers in *Zamia* (Cycadales). Caryologia 33:419–428.

——— 1986 *Zamia chigua*, a case of mistaken identity? Fairchild Trop Gard Bull 41:6–13.

Norstog KJ, TJ Nichols 1997 The biology of the cycads. Cornell University Press, Ithaca, NY.

O'Brien CW, W Tang 2015 Revision of the New World cycad weevils of the subtribe Allocorynina, with description of two new genera and three new subgenera (Coleoptera: Belidae: Oxycoryninae). Zootaxa 3970:1–87.

O'Dea A, HA Lessios, AG Coates, RI Eytan, SA Restrepo-Moreno, AL Cione, LS Collins, et al 2016 Formation of the Isthmus of Panama. Sci Adv 2:1.

Olson K, R Gorelick 2011 Chromosomal fission accounts for small-scale radiations in *Zamia* (Zamiaceae; Cycadales). Bot J Linn Soc 165:168–185.

Osborne R, M Calonje, KD Hill, L Stanberg, DW Stevenson 2012 The world list of cycads. Mem N Y Bot Gard 106:480–510.

Paradis E, J Claude, K Strimmer 2004 APE: Analyses of phylogenetics and evolution in R language. Bioinformatics 20:289–290.

Pérez-Farrera MA, AP Vovides, R Martínez-Camilo, N Martínez-Meléndez, H Gómez-Domínguez, S Galicia-Castellanos 2012 *Zamia grijalvensis* sp. nov. (Zamiaceae, Cycadales) from Chiapas, Mexico with notes on hybridization and karyology. Nord J Bot 30:565–570.

Pérez-Farrera MA, AP Vovides, C Ruiz-Castillejos, S Galicia, A Cibrián-Jaramillo, S López 2016 Anatomy and morphology suggest a hybrid origin of *Zamia katzeriana* (Zamiaceae). Phytotaxa 2016 270:161–181.

Pybus OG, PH Harvey 2000 Testing macro-evolutionary models using incomplete molecular phylogenies. Proc R Soc B 267:2267–2272.

Rabosky DL 2006 LASER: a maximum likelihood toolkit for detecting temporal shifts in diversification rates from molecular phylogenies. Evol Bioinform Online 2:247–250.

——— 2014 Automatic detection of key innovations, rate shifts, and diversity-dependence on phylogenetic trees. PLoS ONE 9:e89543.

——— 2018 Phylogenies and diversification rates: variance cannot be ignored. Syst Biol 0:1–13.

Rabosky DL, AH Hurlbert 2015 Species richness at continental scales is dominated by ecological limits. Am Nat 185:572–583.

Rai HS, HE O'Brien, PA Reeves, RG Olmstead, SW Graham 2003 Inference of higher-order relationships in the cycads from a large chloroplast data set. Mol Phylogenet Evol 29:350–359.

Rambaut A 2012 FigTree v1. 4. Molecular evolution, phylogenetics and epidemiology. University of Edinburgh, Institute of Evolutionary Biology, Edinburgh.

Rambaut A, MA Suchard, D Xie, AJ Drummond 2014 Tracer v1. 6. http://treebioedacuk/software/tracer/.

Ree RH, I Sanmartín 2018 Conceptual and statistical problems with the DEC+J model of founder-event speciation and its comparison with DEC via model selection. J Biogeogr 45:741–749.

Regel E 1876 Cycadearum, generum specierumque revisio. Acta Hort Petropol 4:275–320.

Revell LJ 2012 phytools: an R package for phylogenetic comparative biology (and other things). Methods Ecol Evol 3:217–223.

Sabato S 1990 West Indian and South American cycads. Mem N Y Bot Gard 57:173–185.

Salas-Leiva DE, AW Meerow, M Calonje, J Francisco-Ortega, MP Griffith, K Nakamura, V Sanchez, L Knowles, D Knowles 2017 Shifting Quaternary migration patterns in the Bahamian archipelago: evidence from the *Zamia pumila* complex at the northern limits of the Caribbean island biodiversity hotspot. Am J Bot 104:757–771.

Salas-Leiva DE, AW Meerow, M Calonje, MP Griffith, J Francisco-Ortega, K Nakamura, DW Stevenson, CE Lewis, S Namoff 2013 Phylogeny of the cycads based on multiple single-copy nuclear genes: congruence of concatenated parsimony, likelihood and species tree inference methods. Ann Bot 112:1263–1278.

Salas-Leiva DE, AW Meerow, J Francisco-Ortega, M Calonje, MP Griffith, DW Stevenson, K Nakamura 2014 Conserved genetic regions across angiosperms as tools to develop single-copy nuclear markers in gymnosperms: an example using cycads. Mol Ecol Resour 14:831–845.

Sarich VM 1977 Rates, sample sizes, and the neutrality hypothesis for electrophoresis in evolutionary studies. Nature 265:24–28.

Schuster J 1932 Cycadaceae. Pages 1–168 *in* A Engler, ed. Das Pflanzenreich. Vol IV, Pt I. Engelmann, Leipzig.

Schutzman B 1984 A new species of *Zamia* L. (Zamiaceae, Cycadales) from Chiapas, Mexico. Phytologia 55:299–303.

Schutzman B, AP Vovides 1998 A new *Zamia* (Zamiaceae, Cycadales) from eastern Chiapas, Mexico. Novon 8:441–446.

Schutzman B, AP Vovides, B Dehgan 1988 Two new species of *Zamia* (Zamiaceae, Cycadales) from southern Mexico. Bot Gaz 149:347–360.

Sclater PL 1858 On the general geographical distribution of the members of the Class Aves. J Linn Soc Lond Zool 2:130–136.

Smith BT, J Klicka 2010 The profound influence of the Late Pliocene Panamanian uplift on the exchange, diversification, and distribution of New World birds. Ecography 33:333–342.

Stevenson D, S Sabato, A Moretti, P De Luca 1998 What is *Zamia fischeri* Miquel? Delpinoa, NS, 37–38:9–7.

Stevenson DW 1987 Again the West Indian zamias. Fairchild Trop Gard Bull 42:23–27.

——— 1993 The Zamiaceae in Panama with comments on phytogeography and species relationships. Brittonia 45:1–16.

——— 2001 Flora de Colombia. Monografia No. 21. Orden Cycadales. Instituto de Ciencias Natural, Universidad Nacional de Colombia, Bogota D.C., Colombia.

——— 2004 Cycads of Colombia. Bot Rev 70:194–234.

Swofford DL 2003 PAUP*. Phylogenetic Analysis Using Parsimony (*and other methods). Version 4. Sinauer, Sunderland, MA.

Tang W 1989 Seed dispersal in the cycad *Zamia pumila* in Florida. Can J Bot 67:2066–2070.

——— Seed dispersal and reproductive effort in *Zamia pumila*. Pages 148–157 *in* DW Stevenson, K Norstog, eds. The biology, structure, and systematics of the cycadales Proceedings of Cycad 90, the second international conference on cycad biology. Palm and Cycad Societies of Australia, Milton, Queensland.

Taylor AS, JL Haynes, G Holzman 2008 Taxonomical, nomenclatural and biogeographical revelations in the *Zamia skinneri* complex of Central America (Cycadales: Zamiaceae). Bot J Linn Soc 158: 399–429.

Toledo VM 1982 Pleistocene changes of vegetation in tropical Mexico. Pages 93–111 *in* GT Prance, ed. Biological diversification in the tropics. Columbia University Press, New York.

Treutlein J, M Wink 2002 Molecular phylogeny of cycads inferred from *rbcL* sequences. Naturwissenschaften 89:221–225.

Turland NJ, JH Wiersema, FR Barrie, W Greuter, DL Hawksworth, PS Herendeen, S Knapp, et al 2018 International Code of Nomenclature for algae, fungi, and plants (Shenzhen Code) adopted by the Nineteenth International Botanical Congress Shenzhen, China, July 2017. Regnum Vegetabile 159. Koeltz Botanical Books, Glashütten, Germany. https://doi.org/10.12705/Code.2018.

van Gestel J-P, P Mann, JF Dolan, NR Grindlay 1998 Structure and tectonics of the upper Cenozoic Puerto Rico-Virgin Islands carbonate platform as determined from seismic reflection studies. J Geophys Res: Solid Earth 103:30505–30530.

Vovides AP 1983 Systematic studies on the Mexican Zamiaceae. I. Chromosome numbers and karyotypes. Am J Bot 70:1002–1006.

Vovides AP, M Olivares 1996 Karyotype polymorphism in the cycad *Zamia loddigesii* (Zamiaceae) of the Yucatan Peninsula, Mexico. Bot J Linn Soc 120:77–83.

Wallace AR 1878 Tropical nature, and other essays. AMS, New York.

Walters TW, DS Decker-Walters 1991 Patterns of allozyme diversity in the West Indies cycad *Zamia pumila* (Zamiaceae). Am J Bot 78: 436–445.

Webb SD 1976 Mammalian faunal dynamics of the great American interchange. Paleobiology 2:220–234.

Weigelt P, MJ Steinbauer, JS Cabral, H Kreft 2016 Late Quaternary climate change shapes island biodiversity. Nature 532:99–102.

Wendel JF, JJ Doyle 1998 Phylogenetic incongruence: window into genome history and molecular evolution. Pages 265–296 *in* DE Soltis, PS Soltis, JJ Doyle, eds. Molecular systematics of plants II: DNA sequencing. Springer, Boston.

Whitlock BA, AM Hale, PA Groff 2010 Intraspecific inversions pose a challenge for the *trnH-psbA* plant DNA barcode. PLoS ONE 5: e11533.

Yang SL, AW Meerow 1996 The *Cycas pectinata* (Cycadaceae) complex: genetic structure and gene flow. Int J Plant Sci 157:468–483.

Yessoufou K, SO Bamigboye, BH Daru, M van der Bank 2014 Evidence of constant diversification punctuated by a mass extinction in the African cycads. Ecol Evol 4:50–58.

Yu Y, AJ Harris, C Blair, X He 2015 RASP (Reconstruct Ancestral State in Phylogenies): a tool for historical biogeography. Mol Phylogenet Evol 87:46–49.

Yu Y, AJ Harris, XJ He 2010 S-DIVA (statistical dispersal-vicariance analysis): a tool for inferring biogeographic histories. Mol Phylogenet Evol 56:848–850.

Zgurski JM, HS Rai, QM Fai, DJ Bogler, J Francisco-Ortega, SW Graham 2008 How well do we understand the overall backbone of cycad phylogeny? new insights from a large, multigene plastid data set. Mol Phylogenet Evol 47:1232–1237.

Zhang PY, HTW Tan, KH Pwee, PP Kumar 2004 Conservation of class C function of floral organ development during 300 million years of evolution from gymnosperms to angiosperms. Plant J 37:566–577.

Zonneveld BJM, AJ Lindström 2016 Genome sizes for 71 species of *Zamia* (Cycadales: Zamiaceae) correspond with three different biogeographic regions. Nord J Bot 34:744–751.